HZB Helmholtz Zentrum Berlin

SwedNESS: Real-Space Neutron Imaging

Extreme Imaging
fast, large, high-resolution

Nikolay Kardjilov, Ingo Manke, André Hilger,
John Banhart

Motivation

The Olympic motto: **Citius, Altius, Fortius**

Faster, Higher, Stronger

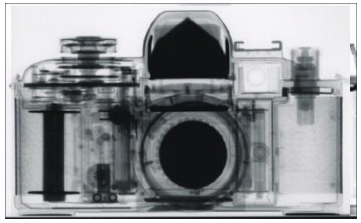

The WCNR motto:

Faster, Higher (Resolution), Larger

Introduction

BER-2 research reactor

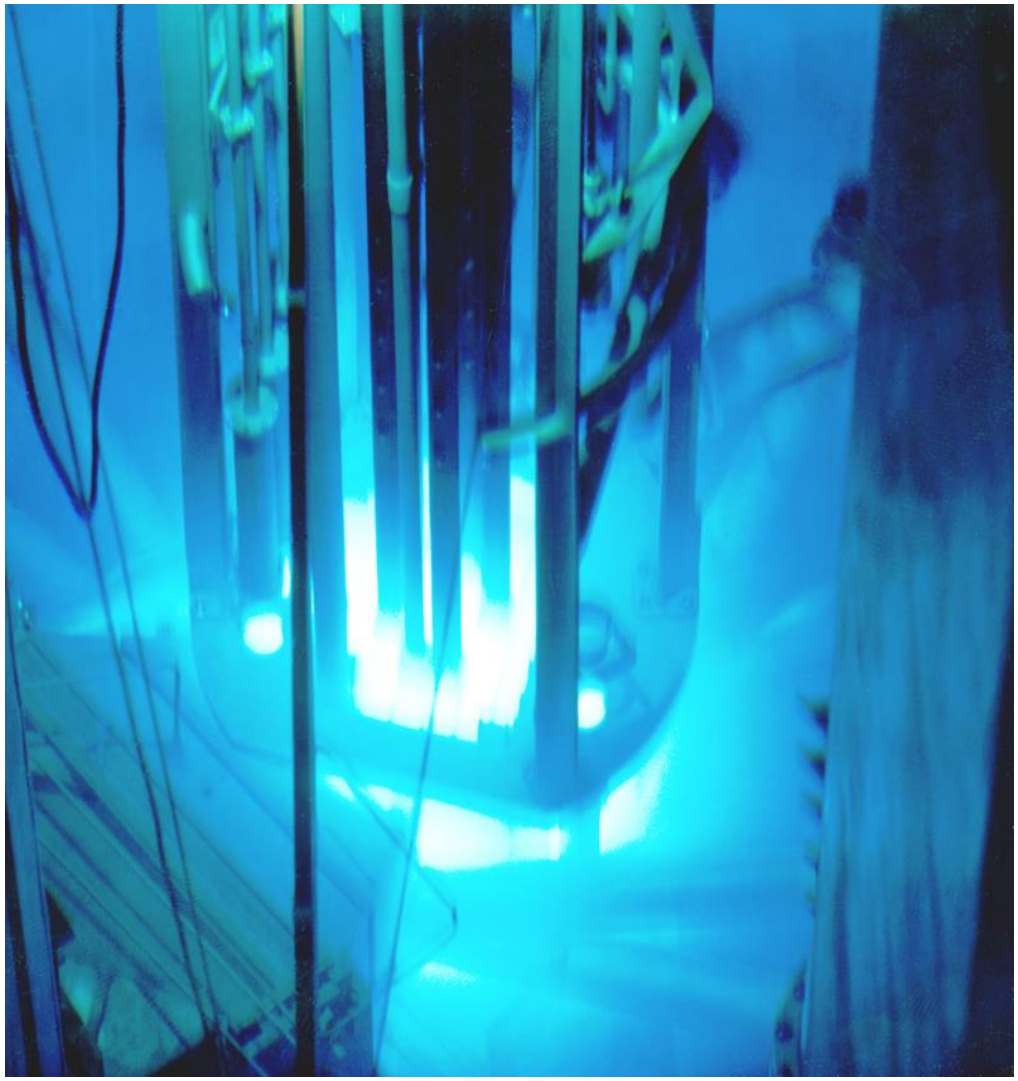

Type: open, light-water-moderated swimming pool reactor

Capacity:
more than 10^{14} neutrons per square centimeter per second in the core 10 megawatts thermal power

The research reactor BER II is a source of neutron beams for around 10 instruments used for structural and materials research.

Introduction

Institute of Applied Materials

Neutron | ***Imaging*** | *Micro CT* | *Synchrotron*

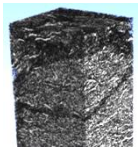

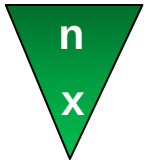

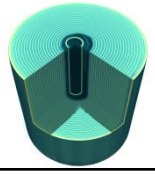

BAM-Line @ BESSY
Synchrotron tomography

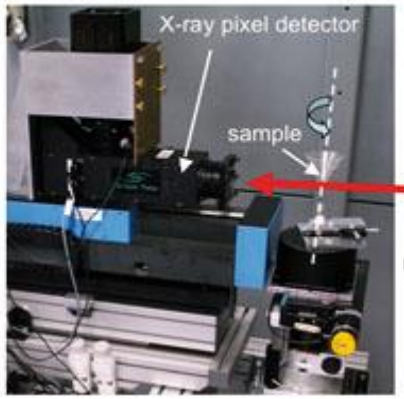

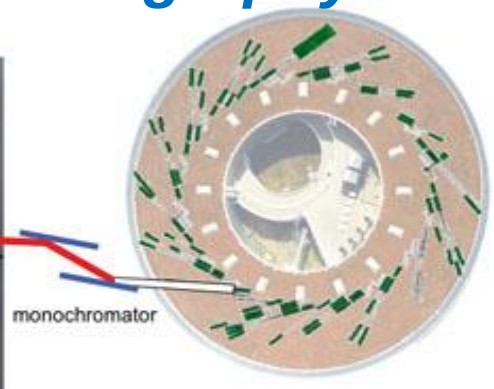

CONRAD-2
neutron tomography

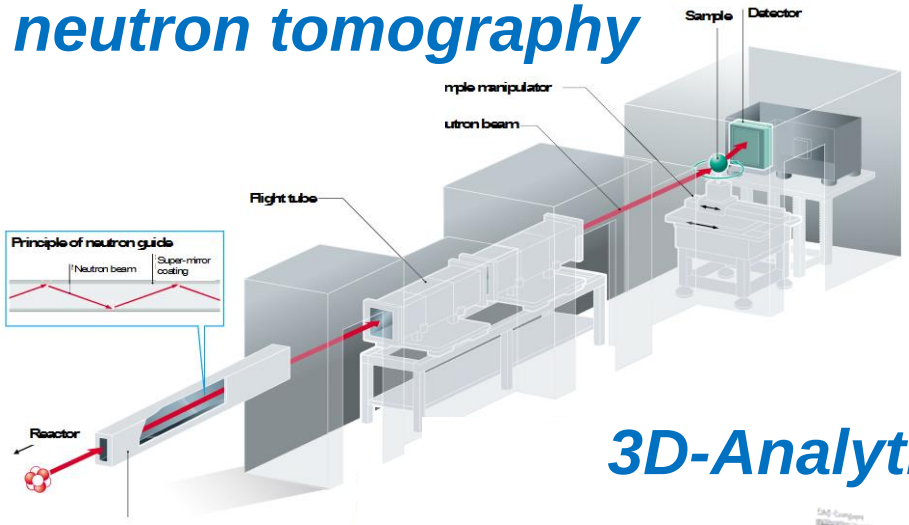

3D-Analytics Lab

MicroCT Lab
X-ray tomography

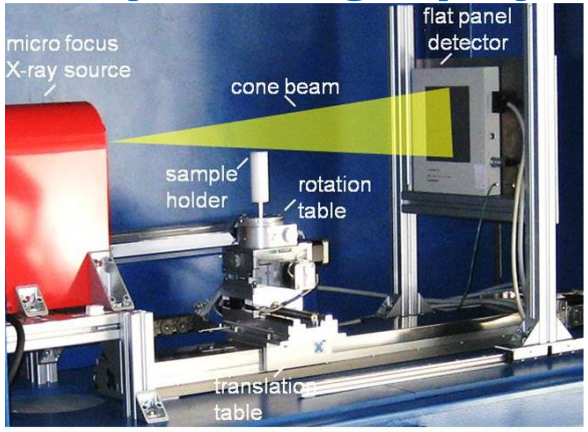

CONRAD-2

Cold neutrons

Wavelength range: 1.5 Å – 10 Å

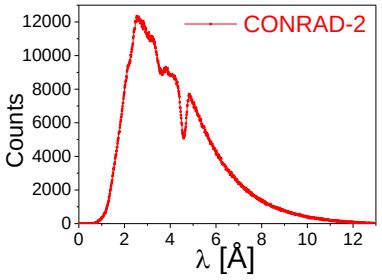

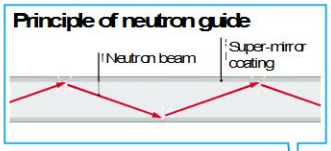

Labs

Micro-CT Lab
3D Data Analytics Lab

Large beam

Beam size: 20 cm x 20 cm

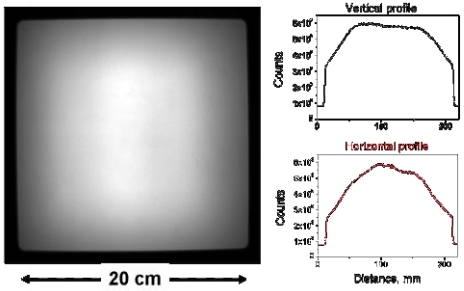

Instrumentation

Neutron polarizers

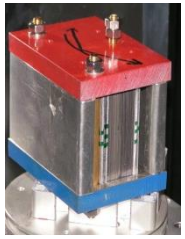

Velocity selector

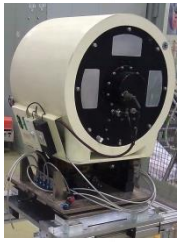

Double-crystal monochromator

Grating interferometry

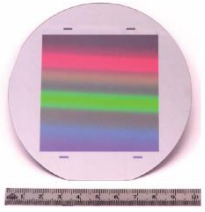

High flux

Flux (guide end): 2.7x10^9 n/cm^{2}s

Guide system: super-mirror coated neutron guide (M=3) with a curvature of 750 m and length of 15 m followed by linear guide section (M=2) with a length of 10 m

Contrast Resolution

- Neutron interaction with matter
  - attenuation contrast
  - diffraction contrast
  - phase/dark-field contrast
  - magnetic contrast
- Beam optimisation
- Detector development

High spatial resolution

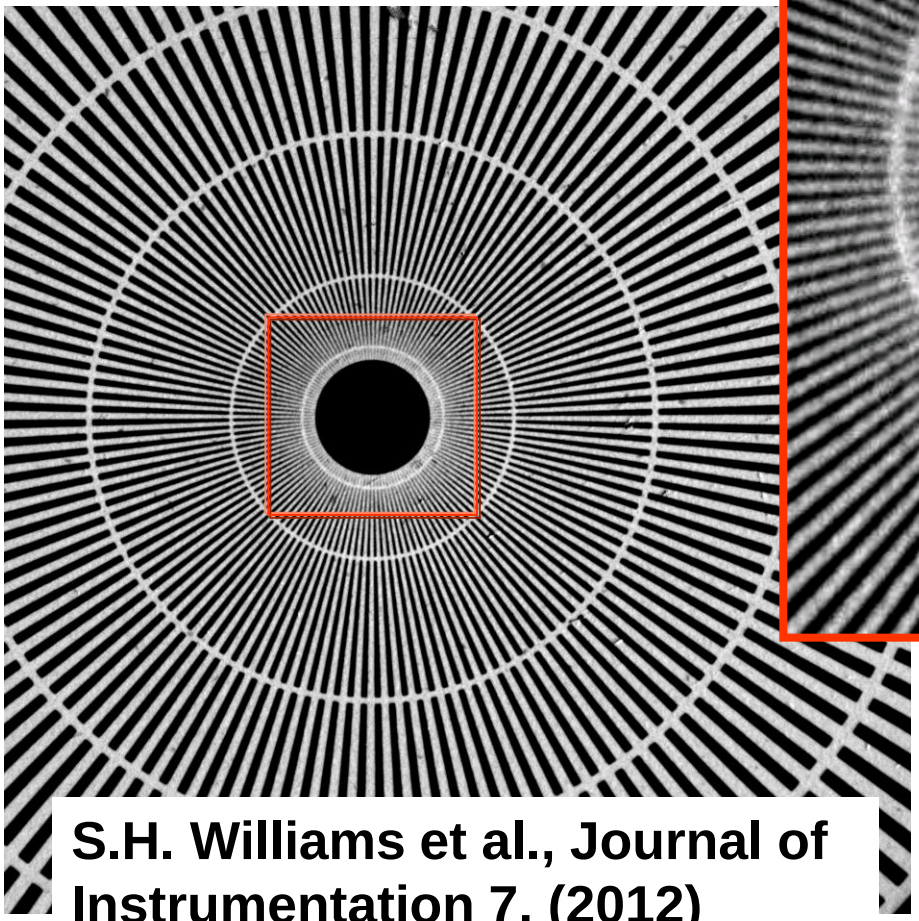

S.H. Williams et al., Journal of Instrumentation 7, (2012)

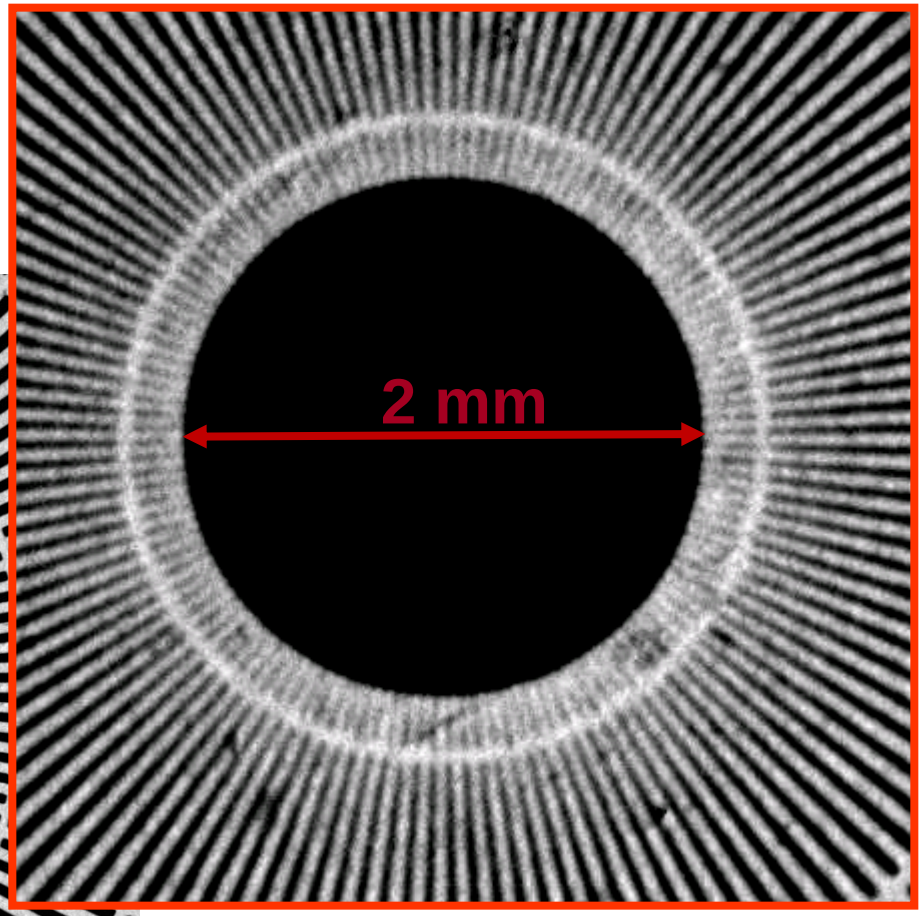

Camera: Andor DW436
Lens system: Magnification
Pixelsize = 3.375 µm
Szintillator: GGG
Resolution: 7.9 µm (63.2 lp/mm)

L/D ratio

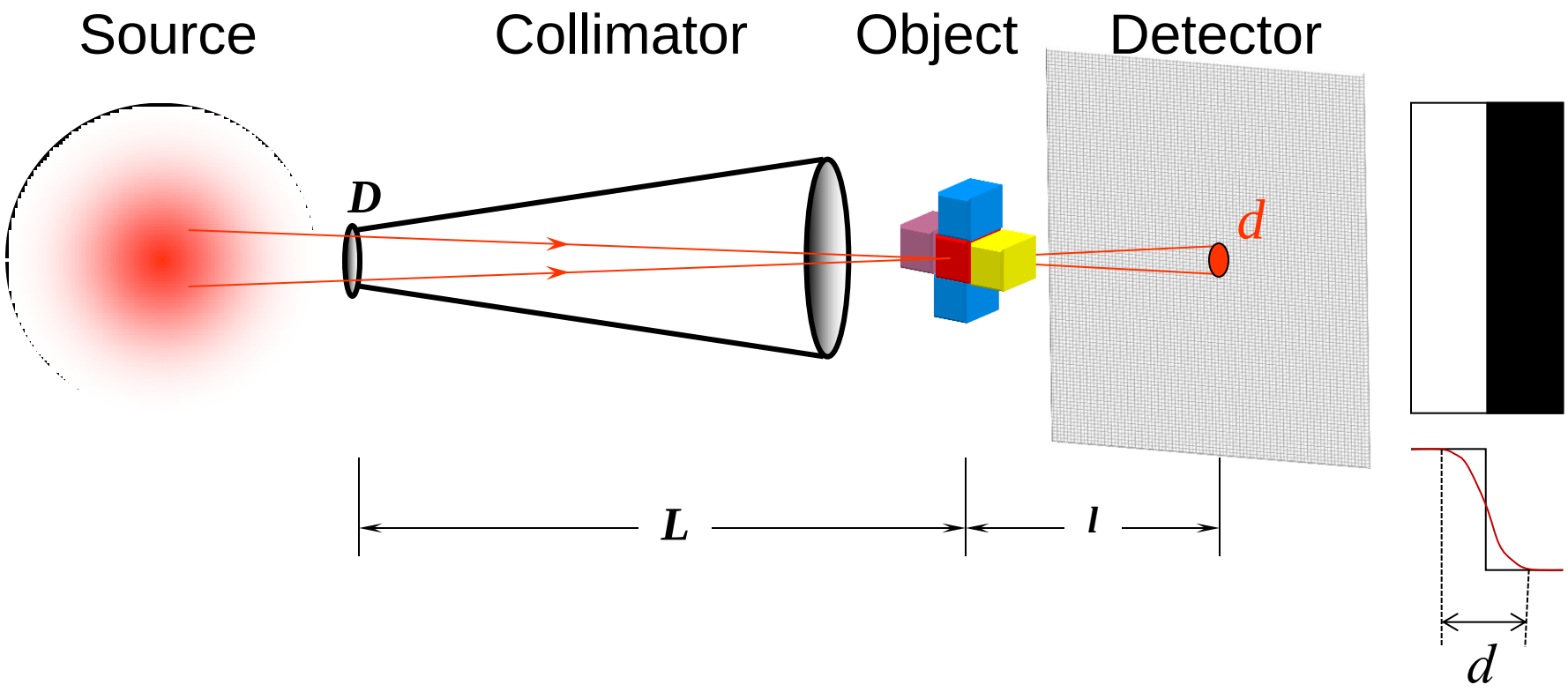

D – Collimator aperture

L – Distance Collimator-Object

l – Distance Object-Detector

$$d = \frac{l}{L/D}$$

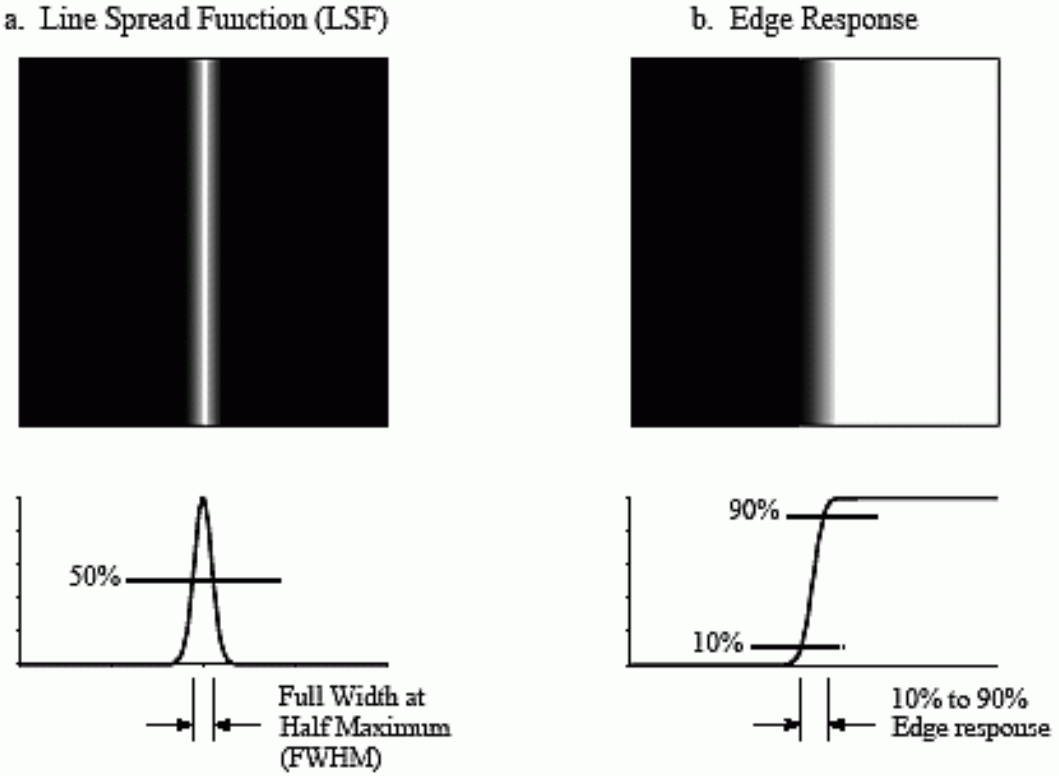

FIGURE 25-3
Line spread function and edge response. The line spread function (LSF) is the derivative of the edge response. The width of the LSF is usually expressed as the Full-Width-at-Half-Maximum (FWHM). The width of the edge response is usually quoted by the 10% to 90% distance.

Spatial resolution

MTF is the *spatial* frequency response of an imaging system or a component; it is the contrast at a given spatial frequency relative to low frequencies.

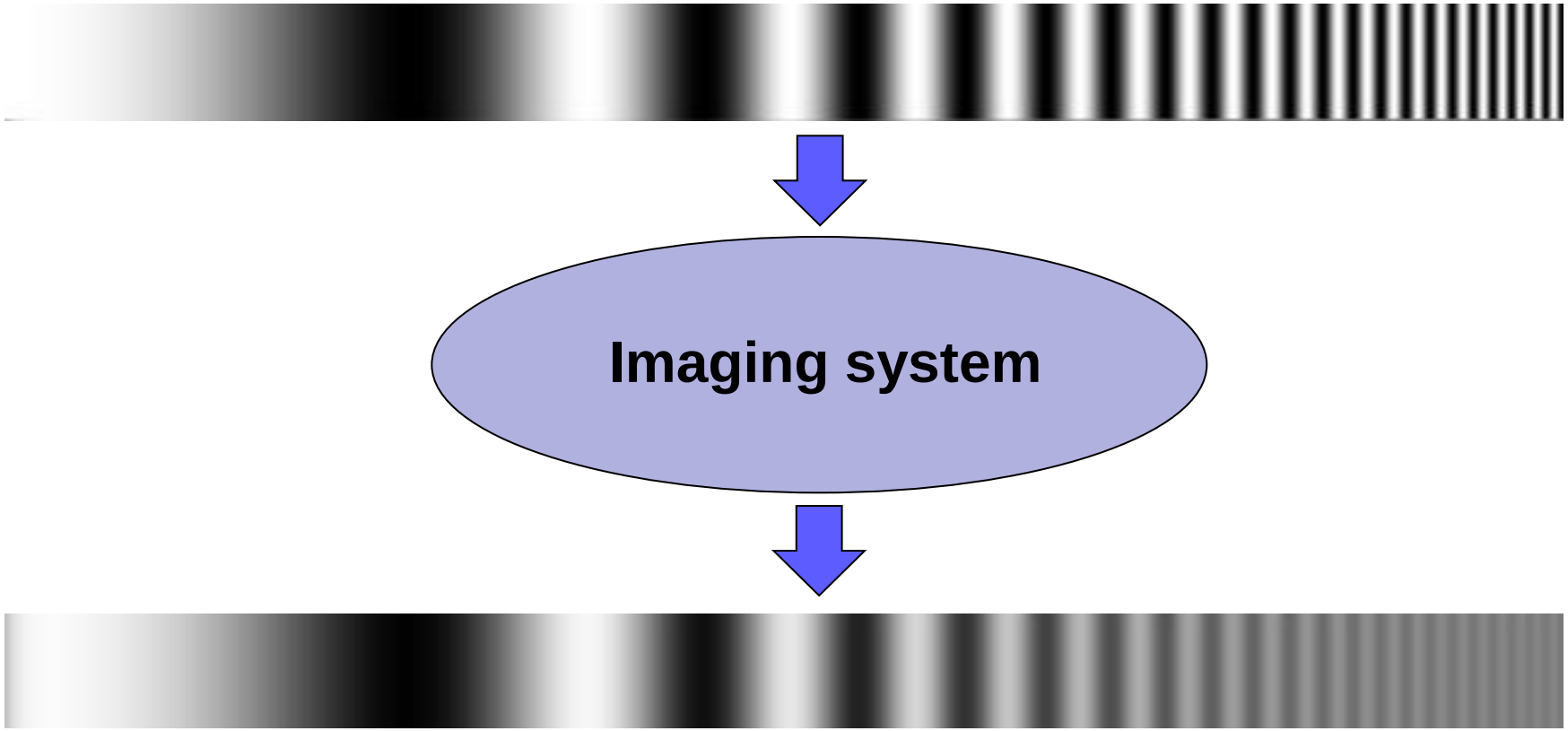

http://www.normankoren.com/Tutorials/MTF.html

Spatial resolution & contrast

Contrast levels

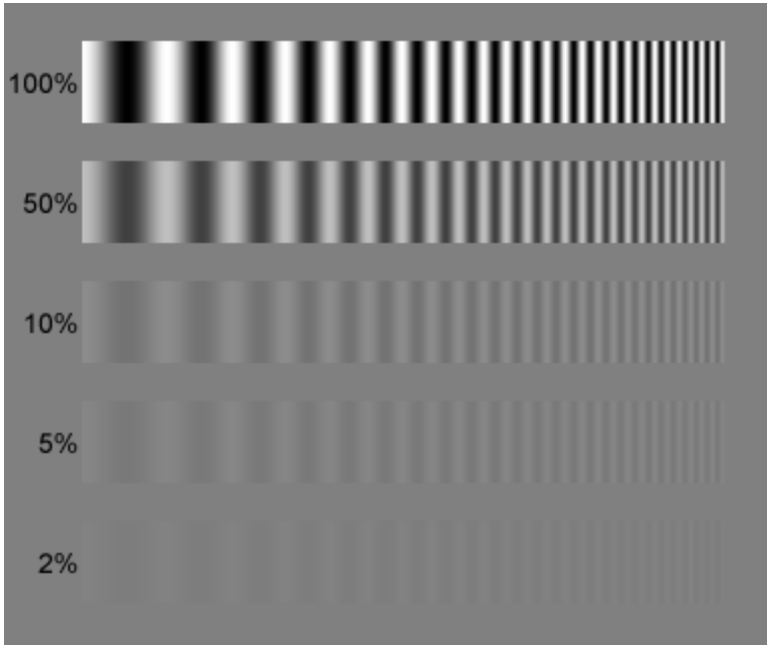

Frequence response: MTF

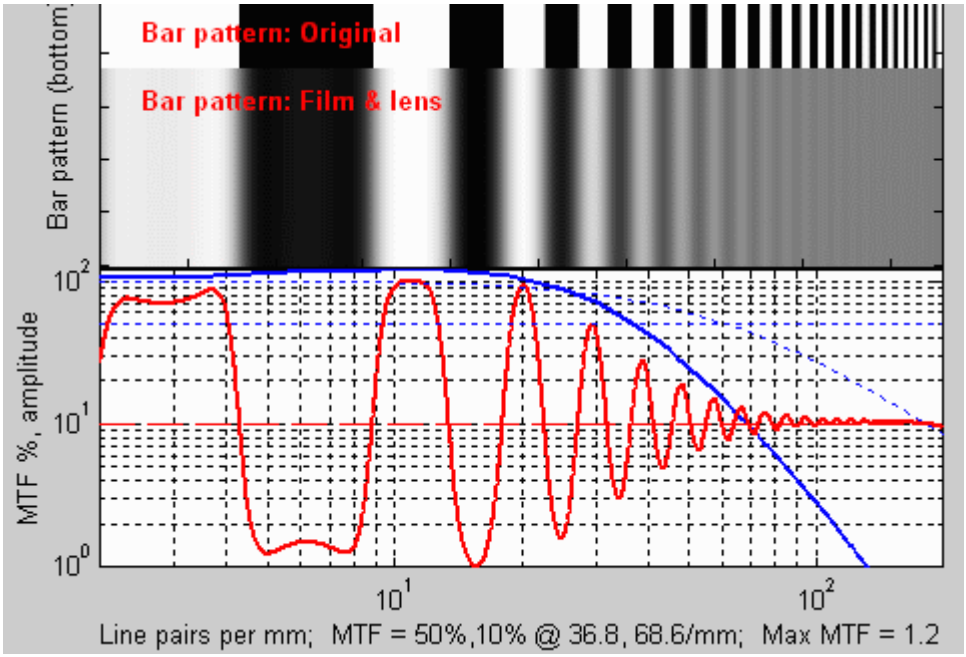

http://www.normankoren.com/Tutorials/MTF.html

Spatial resolution

Scintillator: 5 µm Gadox
Lens system: 200 mm
Pixel size: 15 µm
Exposure time: 150 s

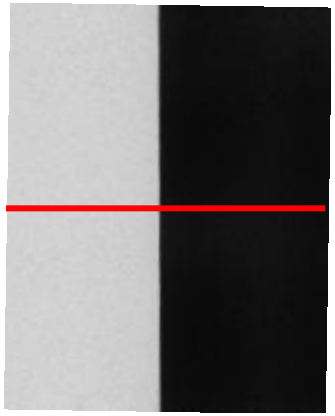

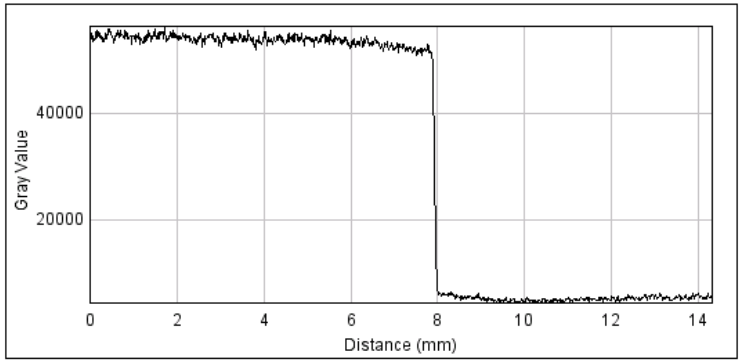

20 lp/mm ~ 25 µm

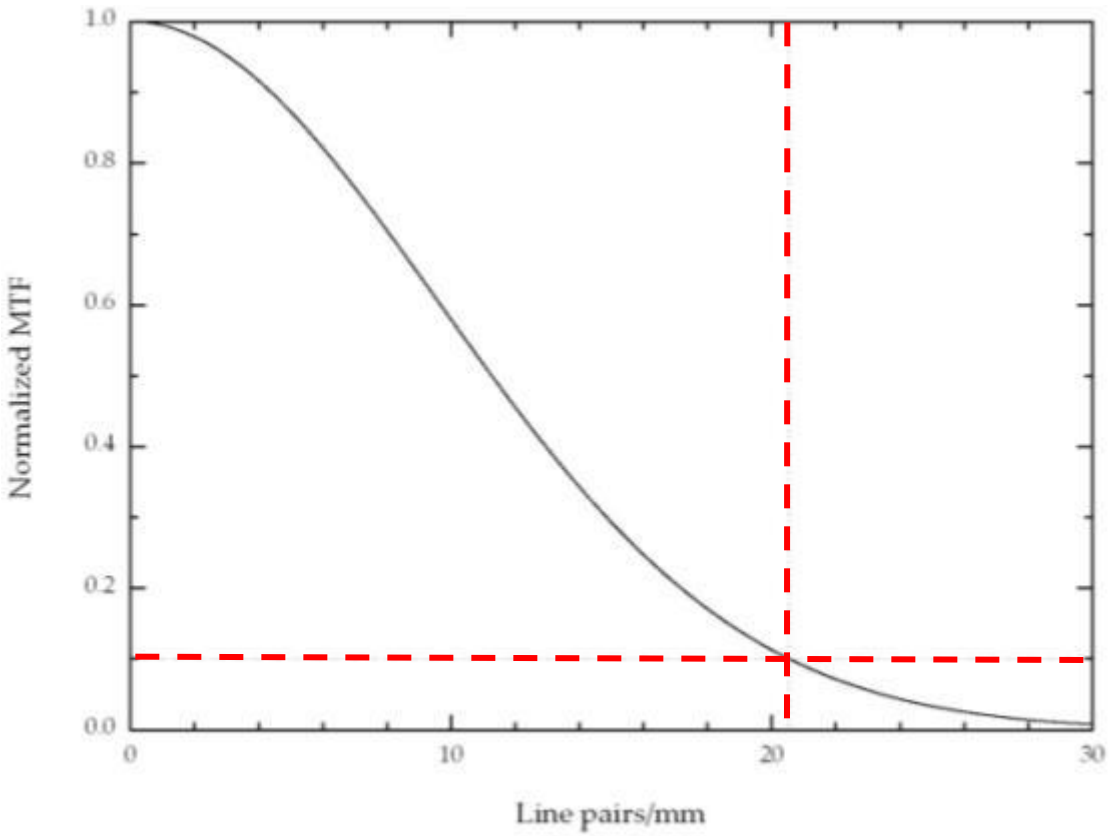

N. Kardjilov, et al. "A highly adaptive detector system for high resolution neutron imaging." *Nuclear Instruments and Methods in Physics Research Section A* 651.1 (2011): 95-99.

High resolution NI

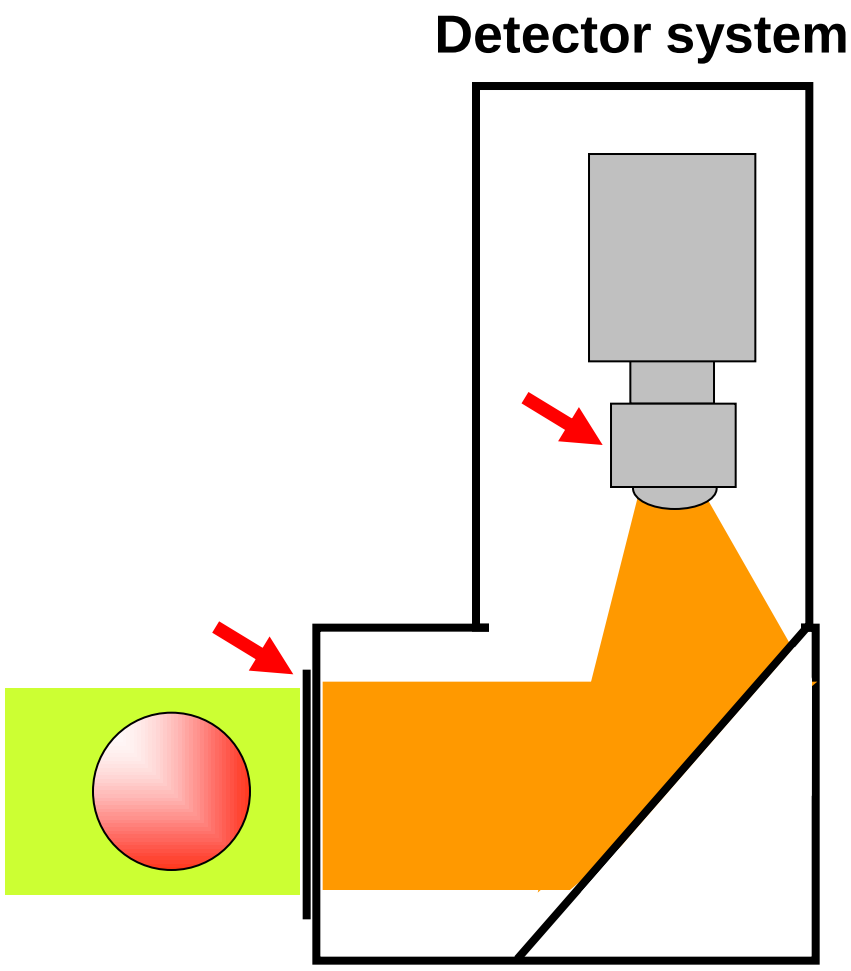

Standard setup (2006)

Scintillator: 200 µm 6LiF
Lens system: 50 mm
Pixel size: 100 µm
Exposure time: 20 s

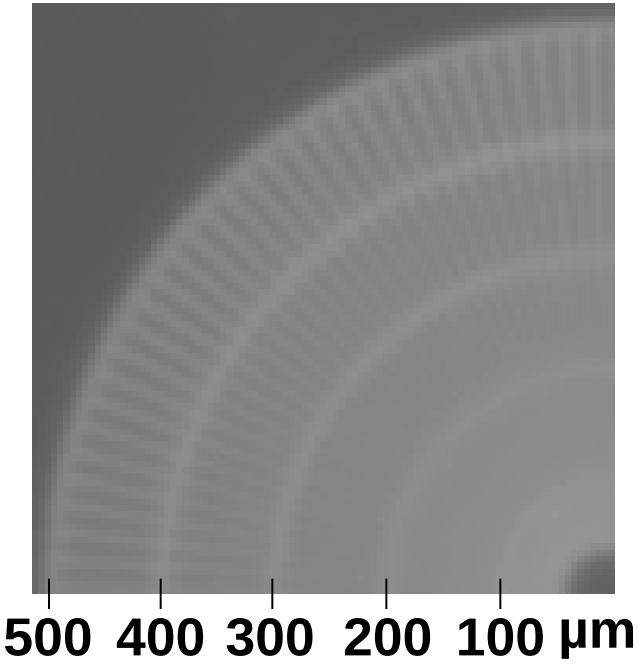

Detector system

CCD camera:
ANDOR DW-436

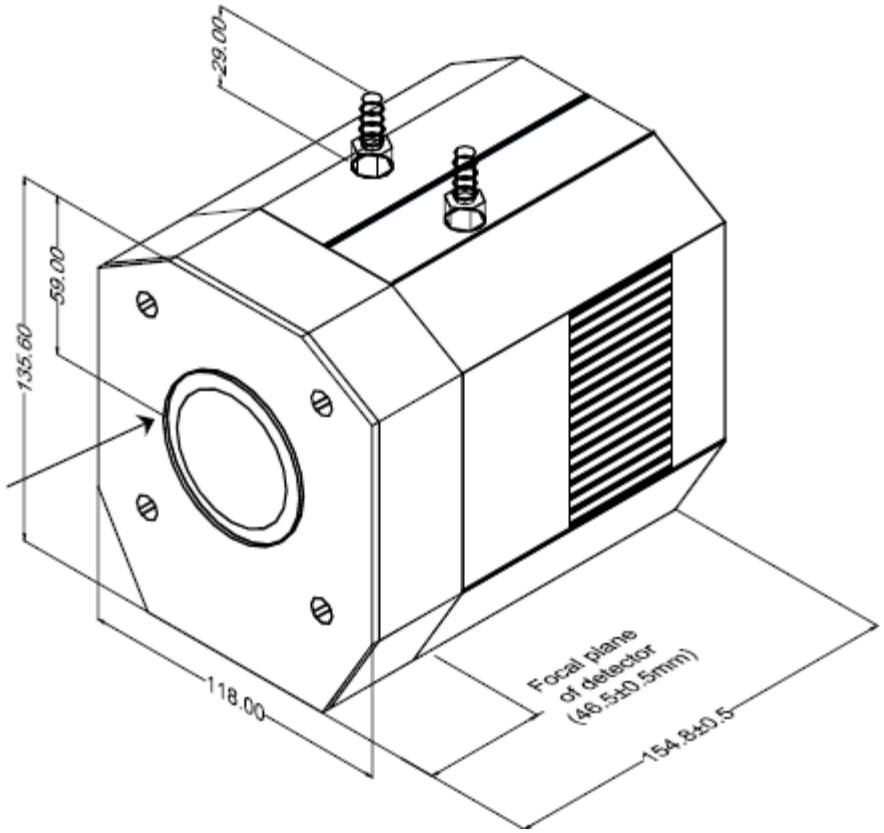

●Sensor	Active Pixels	2048 x 2048	Dummy Pixels*1	50, 50, 0, 0
	Pixel Size (μm²)	13.5	Image Area (mm)	27.6 x 27.6
	Pixel Well Depth (e⁻, typical)	80,000	Register Well Depth (e⁻, typical)*2	600,000
	Linearity (%, maximum)*3	1	Gain (e⁻/count @ 1&2, 16, 32 μs)	2, 1.4, 0.7
	Vertical Clock Speed (μs)	112		

Lens systems

Nikkor Makro-Objektiv - 105 mm - F/2.8

FOV_{max}: 10 cm x 10 cm, pixel size: 50 µm
FOV_{min} : 6 cm x 6 cm, pixel size: 30 µm

Nikon Micro Nikkor 200mm f/4 D (IF) ED

1:1 imaging
FOV_{max}: 2.8 cm x 2.8 cm, pixel size: 13.5 µm

N. Kardjilov, et al. "A highly adaptive detector system for high resolution neutron imaging." *Nuclear Instruments and Methods in Physics Research Section A* 651.1 (2011): 95-99.

Scintillators

neutron detection for imaging

- no direct neutron detection possible
- a secondary nuclear process is needed
  (capture, fission, collision)
- main ***neutron imaging processes*** are using:
  - scintillation
  - photo-luminiscence — by secondary particles + β, γ
  - nuclear track detection
  - chemical excitation
  - collection of charge in semiconductors — from Gd conversion

Capture reactions for thermal / cold neutrons

$^{3}He + {}^{1}n \Rightarrow {}^{3}He + {}^{1}p + 0.77\ MeV$

→ $^{6}Li + {}^{1}n \Rightarrow {}^{3}H + {}^{4}He + 4.79\ MeV$

$^{10}B + {}^{1}n \Rightarrow {}^{7}Li + {}^{4}He + 2.78\ MeV \quad (7\%)$

$\Rightarrow {}^{7}Li^{*} + {}^{4}He + 2.30\ MeV \quad (93\%)$

→ $^{155}Gd + {}^{1}n \Rightarrow {}^{156}Gd + \gamma's + CE's\ (7.9\ MeV)$

$^{157}Gd + {}^{1}n \Rightarrow {}^{158}Gd + \gamma's + CE's\ (8.5\ MeV)$

$^{235}U,\ {}^{239}Pu\ {}^{1}n \Rightarrow$ fission products + 80 MeV

Scintillators

The ZnS+^{6}LiF scintillation screen is the limit of resolution.

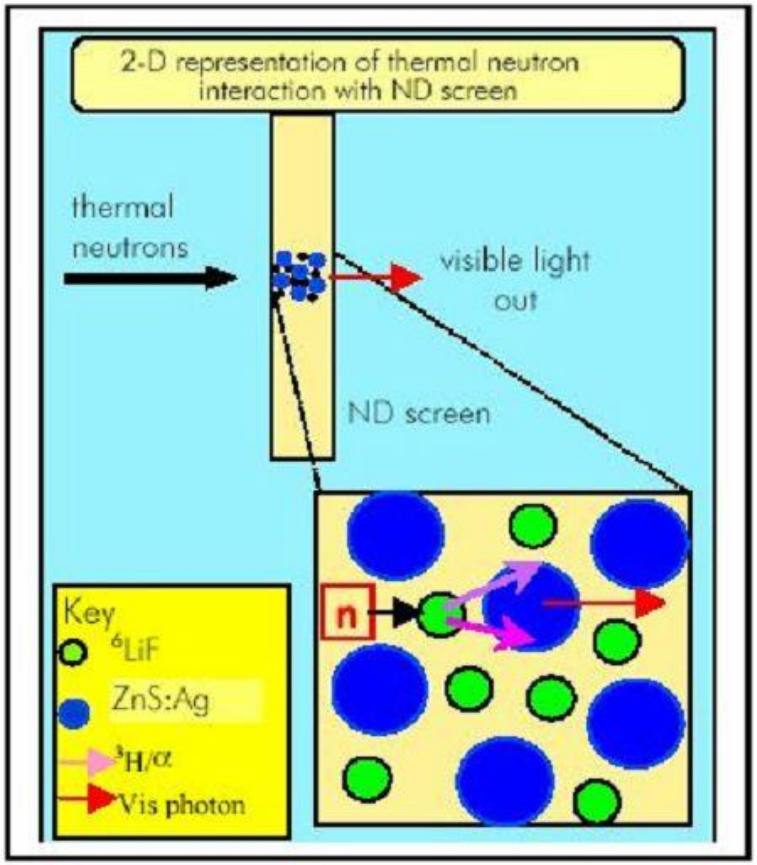

The reaction products of

$^{6}Li(n,\alpha) \rightarrow {}^{3}H + {}^{4}He + 4.7$ MeV

have to be stopped in the ZnS scintillation screen.
Their average range is in the order of 50-80 μm.

About 177,000 photons are generated per detected neutron.

With thinned scintillation screens, we can achieve resolution in the order of 20-30 μm.

Slide courtesy: Dr. Burkhard Schillinger (FRM-II, Munich, Germany)

Scintillators, effect of thickness

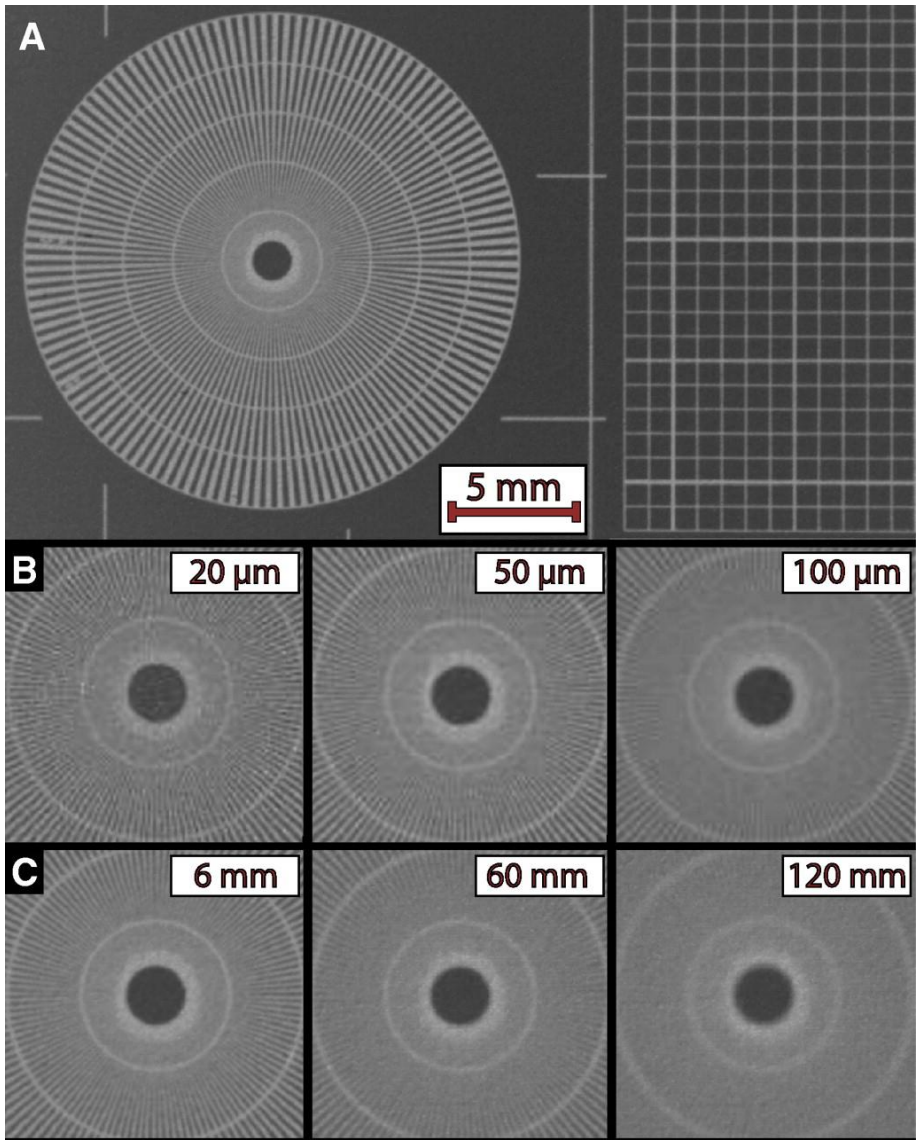

(A) A radiograph of the Siemens star test pattern used to study the effect of scintillator thickness, exposure time, and impact of geometrical blurring.
(B) Images showing the center of the Siemens star for scintillators of different thicknesses.
(C) The same region imaged by a scintillator of 50 µm thickness. In each image the test pattern is placed further away from the scintillator, resulting in increased geometrical blurring.

K.-U. Hess et al., Advances in high-resolution neutron computed tomography: Adapted to the earth sciences , Geosphere (2011) 7 (6): 1294-1302.

Scintillating screens

Thinner scintillating layers improve the spatial resolution but decrease the efficiency which reflects in longer exposure times:

	Thickness	Att. Coefficient, σ_{total} @1.8Å	Free-mean-path
^{6}LiFZnS:Ag	50 µm	3.1 cm^{-1} (2%)	130 µm
GdO_2S:Tb	10 µm	1500 cm^{-1} (78%)	12 µm

N. Kardjilov, et al. "A highly adaptive detector system for high resolution neutron imaging." *Nuclear Instruments and Methods in Physics Research Section A* 651.1 (2011): 95-99.

Lens systems + scintillators

Standard setup

Scintillator: 200 µm 6LiF
Lens system: 50 mm
Pixel size: 100 µm
Exposure time: 20 s

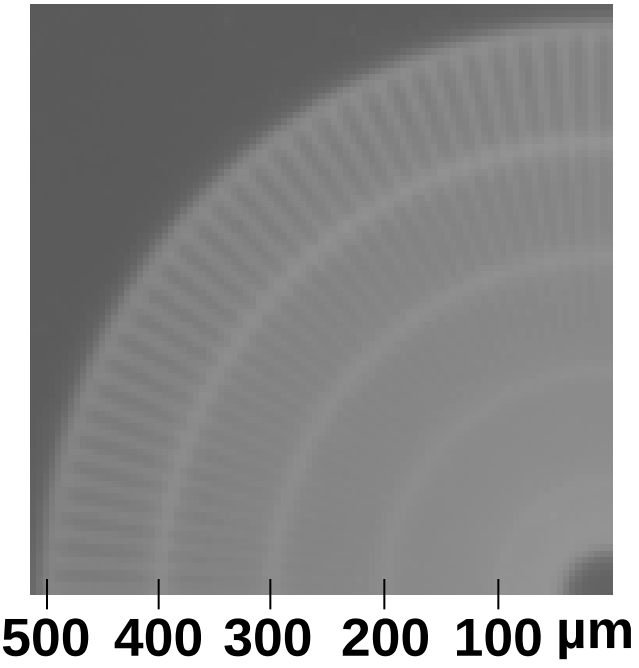

Improved lenses

Scintillator: 200 µm 6LiF
Lens system: 105 mm
Pixel size: 30 µm
Exposure time: 20 s

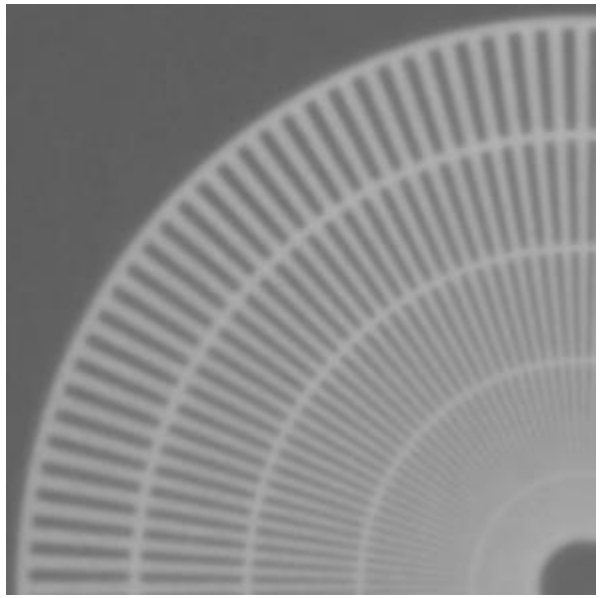

+ Improved screen

Scintillator: 5 µm Gadox
Lens system: 105 mm
Pixel size: 30 µm
Exposure time: 120 s

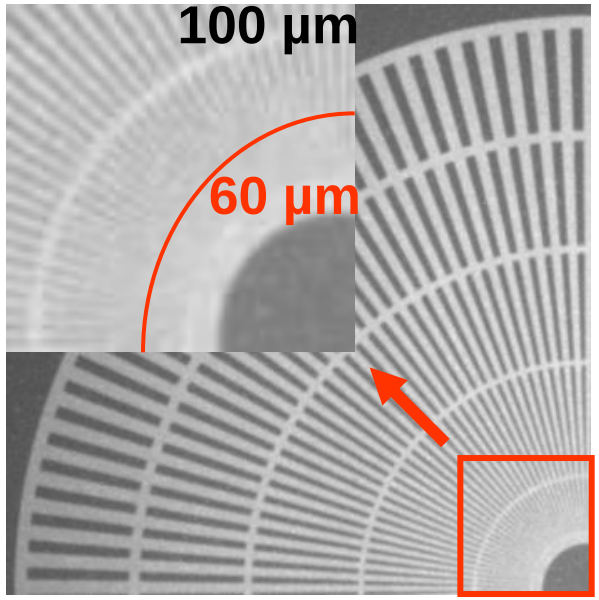

N. Kardjilov, et al. "A highly adaptive detector system for high resolution neutron imaging." *Nuclear Instruments and Methods in Physics Research Section A* 651.1 (2011): 95-99.

Lens systems + scintillators

Scintillator: 5 µm Gadox
Lens system: 105 mm
Pixel size: 30 µm
Exposure time: 120 s

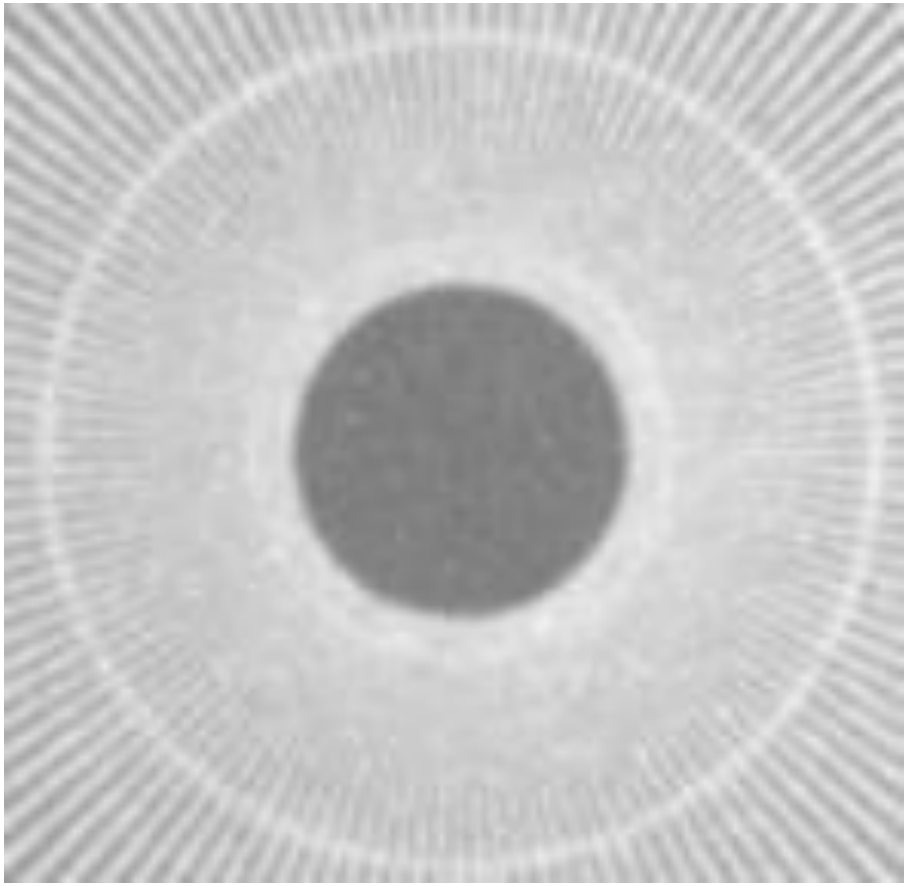

Scintillator: 10 µm Gadox
Lens system: 200 mm
Pixel size: 15 µm
Exposure time: 150 s

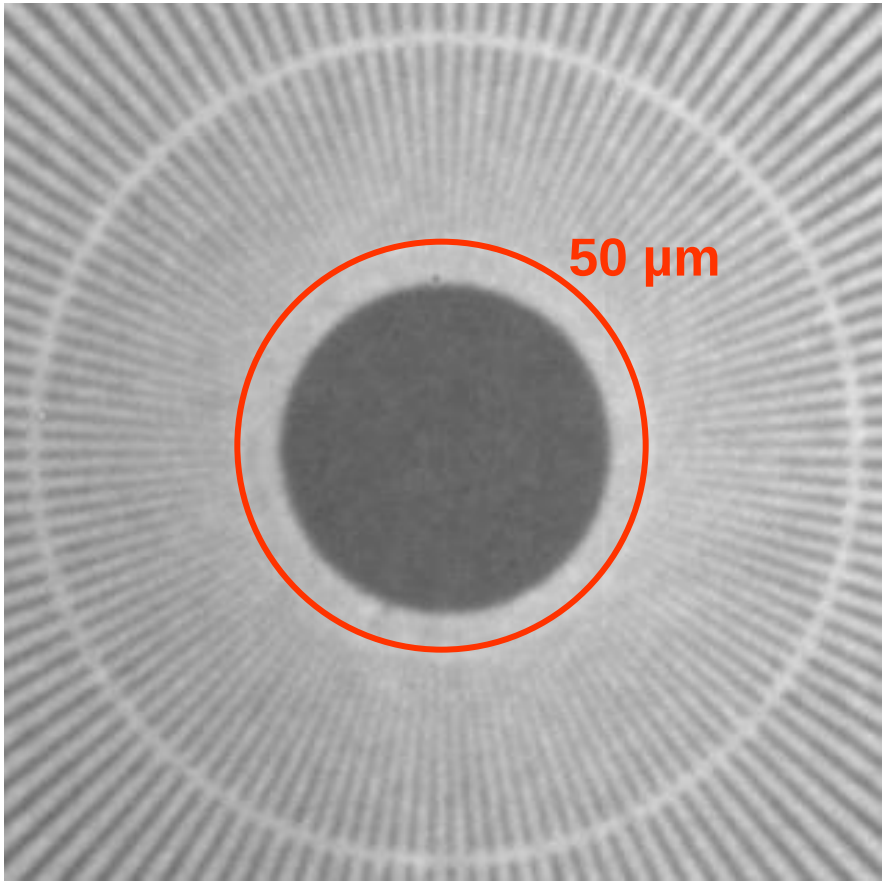

High resolution

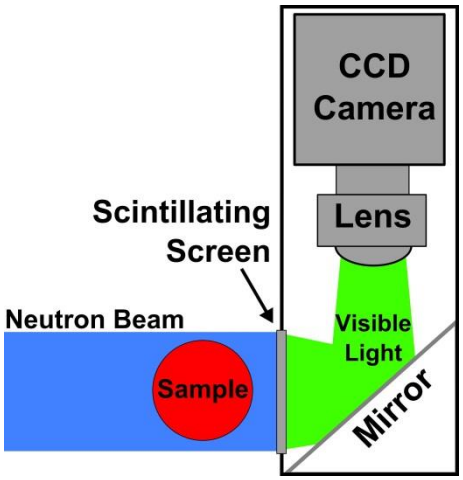

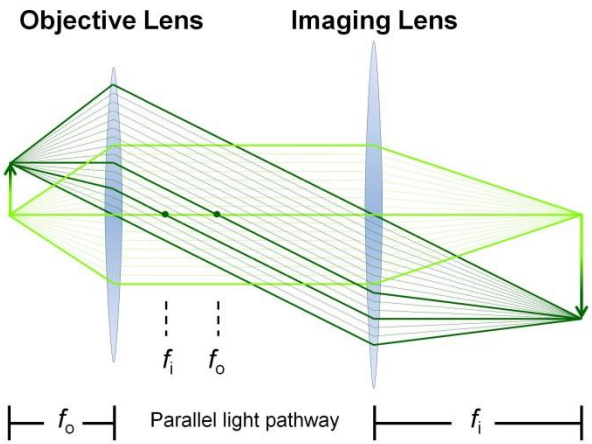

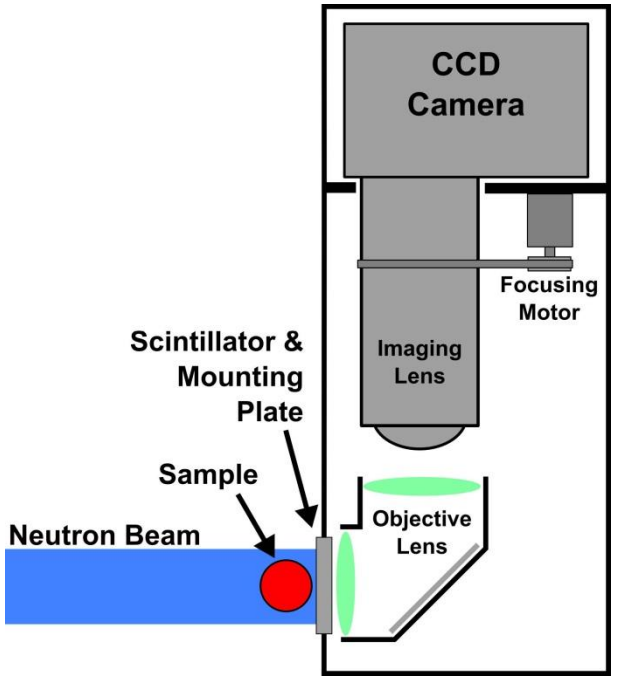

Table 2. Magnification (M), effective pixel size (P_{eff}), Field of View (FOV) and neutron flux of several objective/imaging lens combinations with three available pinhole diameters.

				Neutron flux (n/s/pixel)		
Obj. Lens/Img. Lens	*M*	P_{eff} (μm)	*FOV (mm)*	*D = 3 cm*	*D = 2 cm*	*D = 1 cm*
105 mm / 50 mm	2.10	6.429	13.2 × 13.2	9.9	6.6	2.4
200 mm / 100 mm	2.00	6.750	13.8 × 13.8	10.9	7.3	2.6
200 mm / 50 mm	4.00	3.375	6.9 × 6.9	2.7	1.8	0.7

S. H. Williams et al, J. of Instrumentation (2012)

Spatial Resolution

Camera: Andor DW436
Lens system: Magnification
Pixelsize = 3.375 µm
Szintillator: 5 µm Gadox
Resolution: 7.9 µm (63.2 lp/mm)

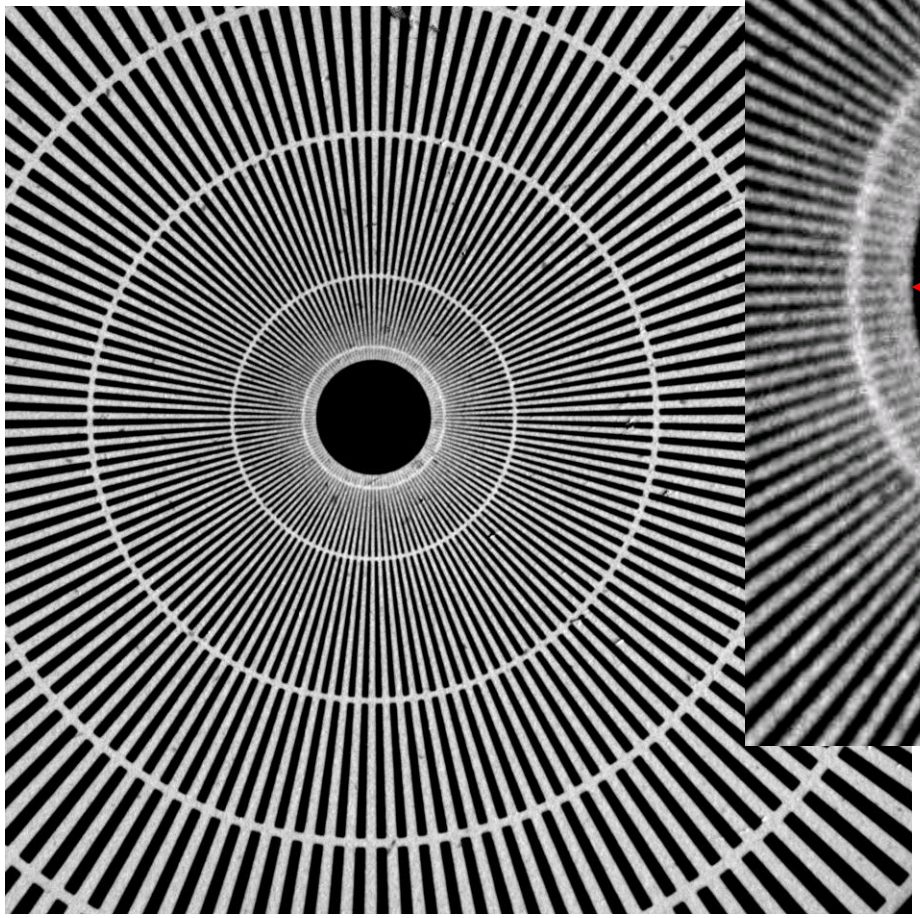

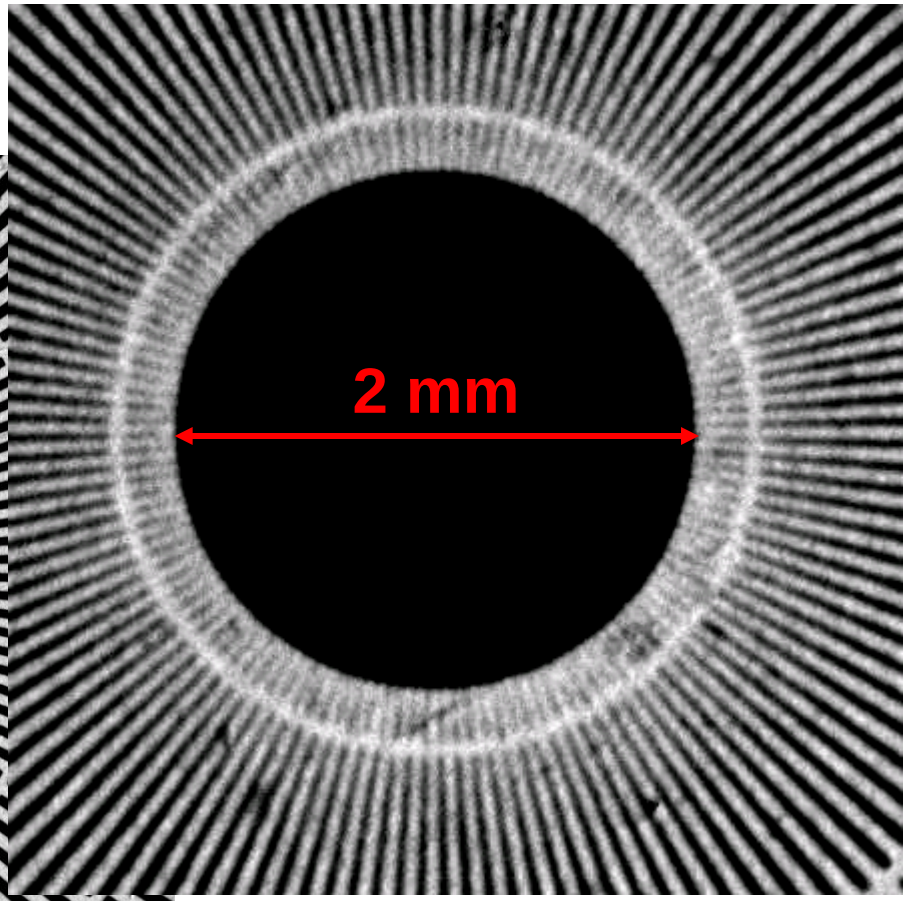

Spatial Resolution

Hydrogen loading of ferritic steel
(A. Griesche, *BAM*, Berlin, Germany)

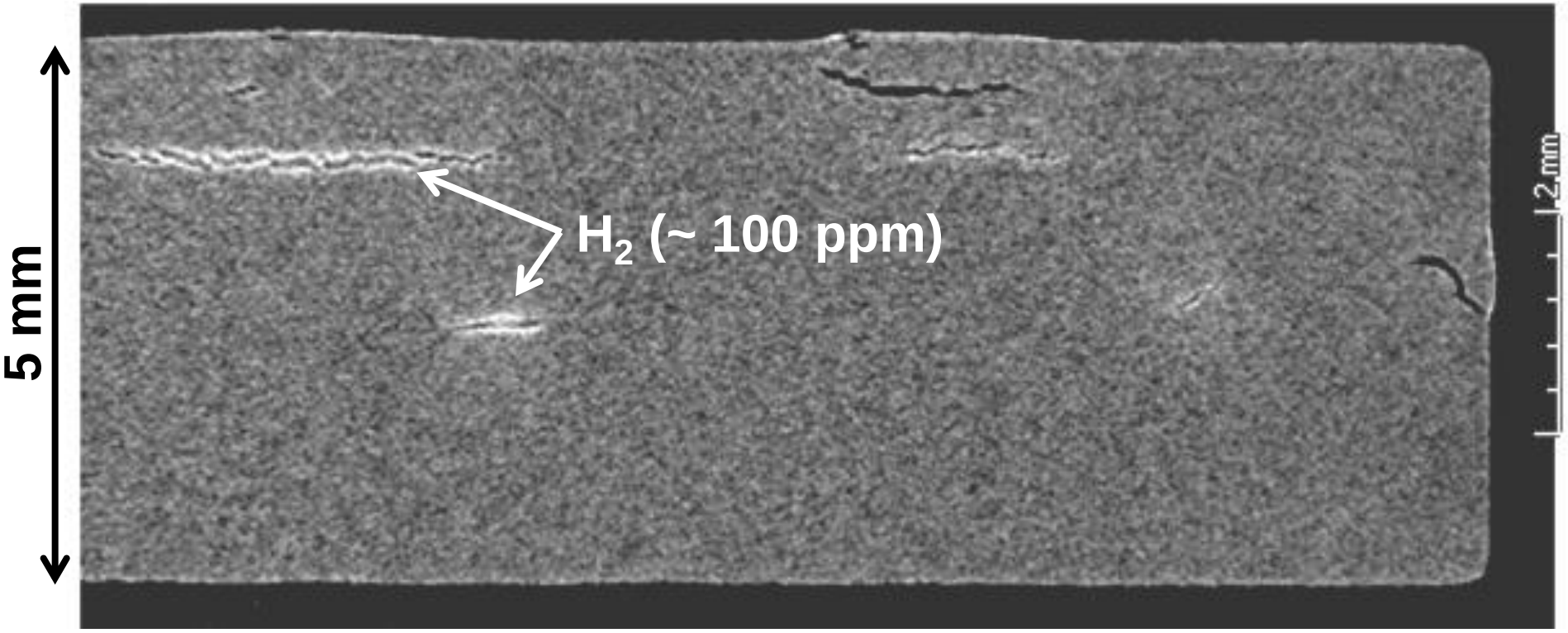

Electrochemically loading

Griesche, Axel, et al. "Three-dimensional imaging of hydrogen blister in iron with neutron tomography." *Acta Materialia* 78 (2014): 14-22.

Attenuation Contrast

Fuel cells

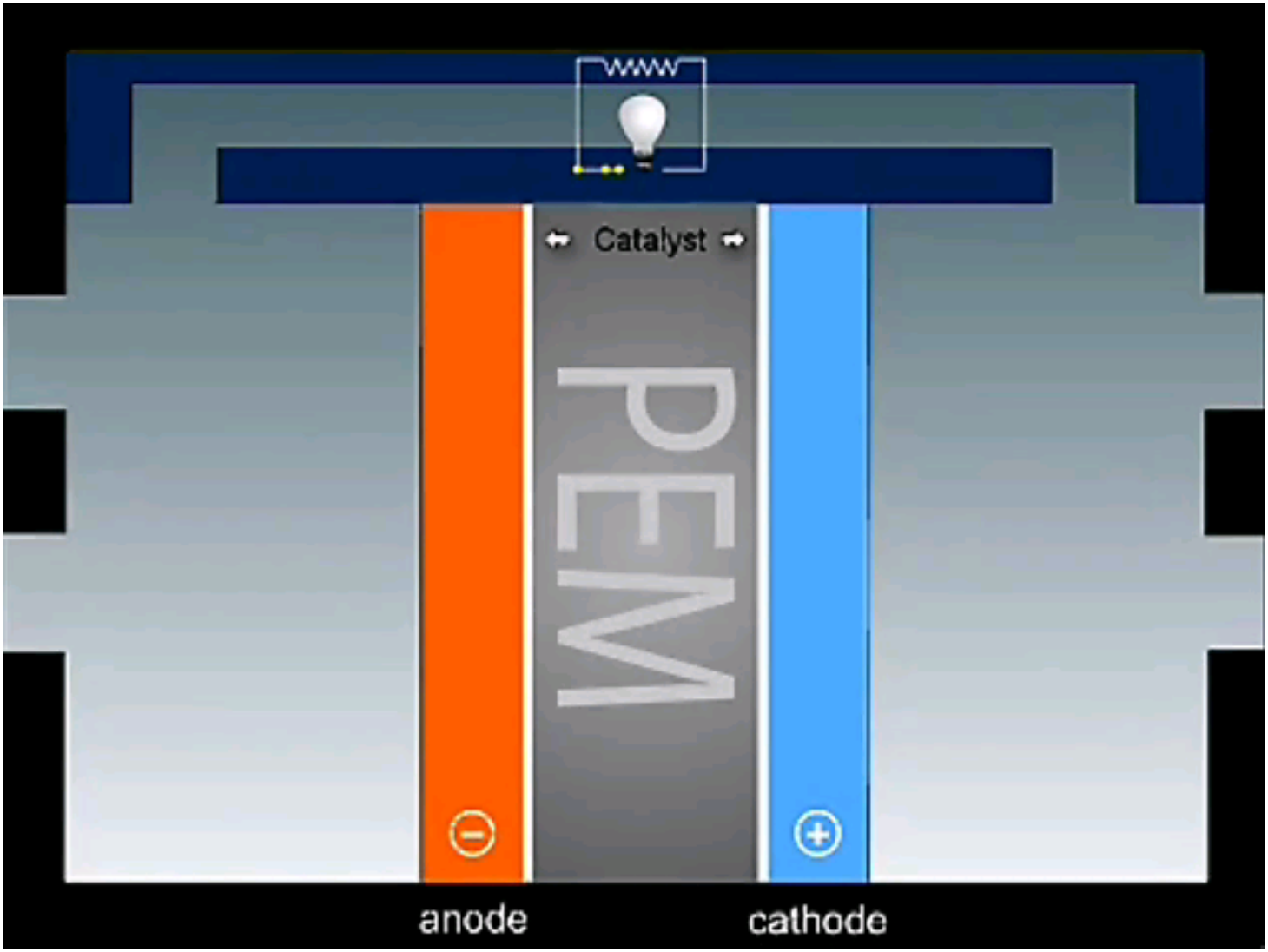

Attenuation Contrast

Fuel cells

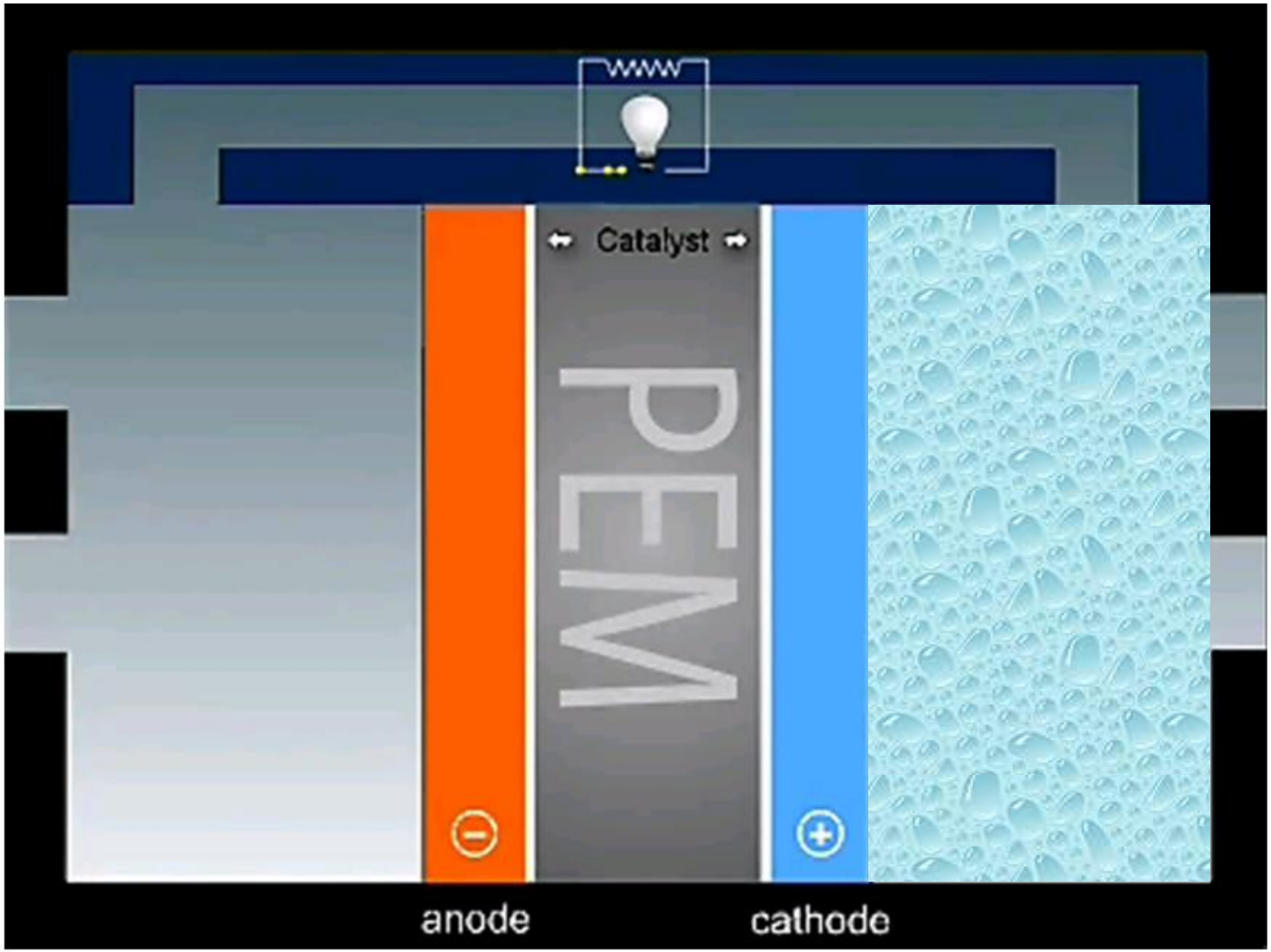

Attenuation Contrast

Fuel Cells

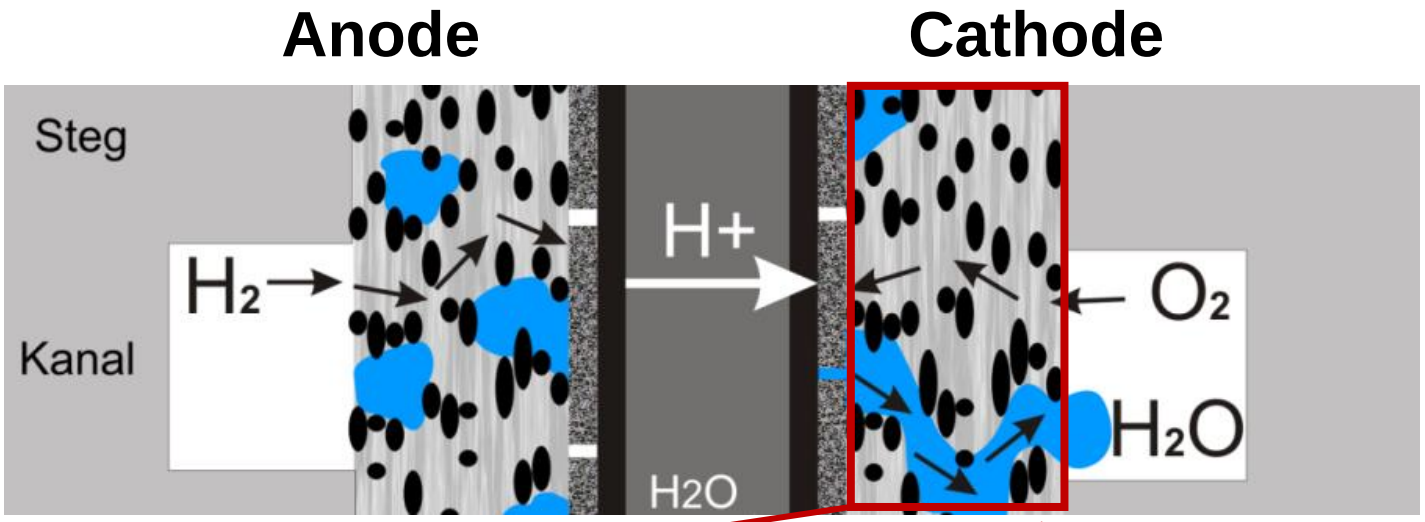

Innovative design

Hydrophobic material

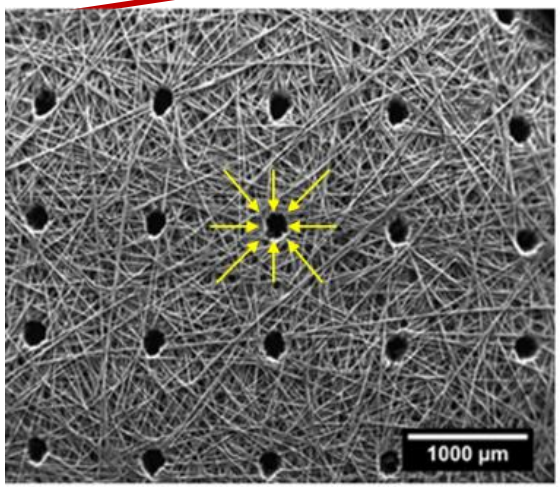

Perforation = Drainage effect

Resolution ?

High resolution

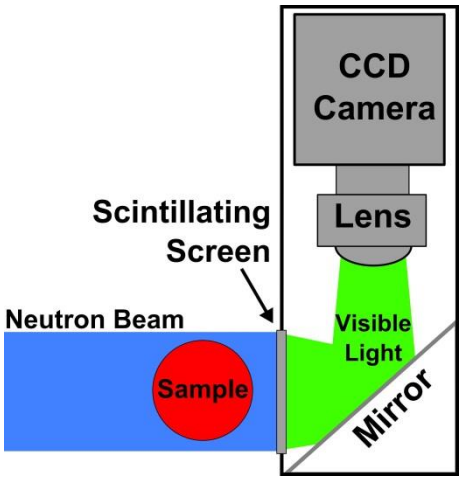

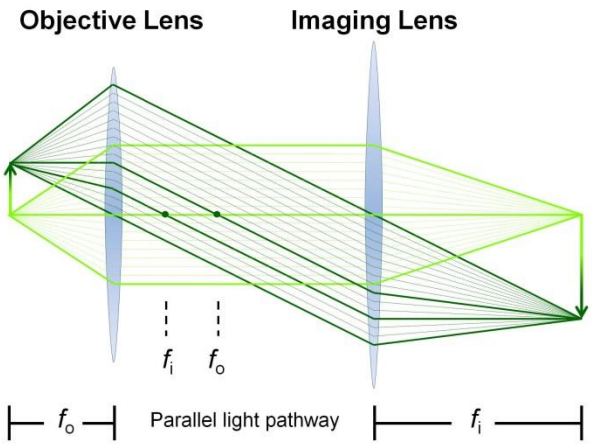

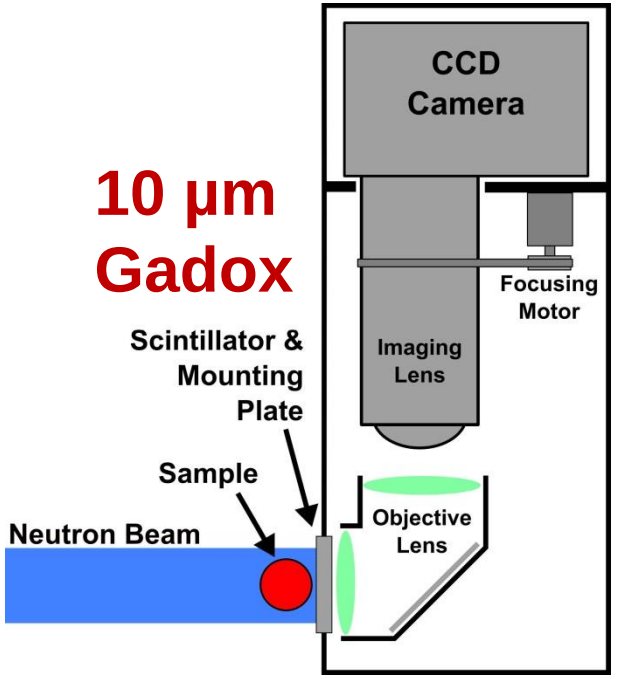

Obj. Lens/Img. Lens	*M*	P_{eff} (µm)	*FOV (mm)*
105 mm / 50 mm	2.10	6.429	13.2 × 13.2
200 mm / 100 mm	2.00	6.750	13.8 × 13.8
200 mm / 50 mm	4.00	3.375	6.9 × 6.9

S. H. Williams et al, J. of Instrumentation (2012)

Attenuation Contrast

Fuel Cells

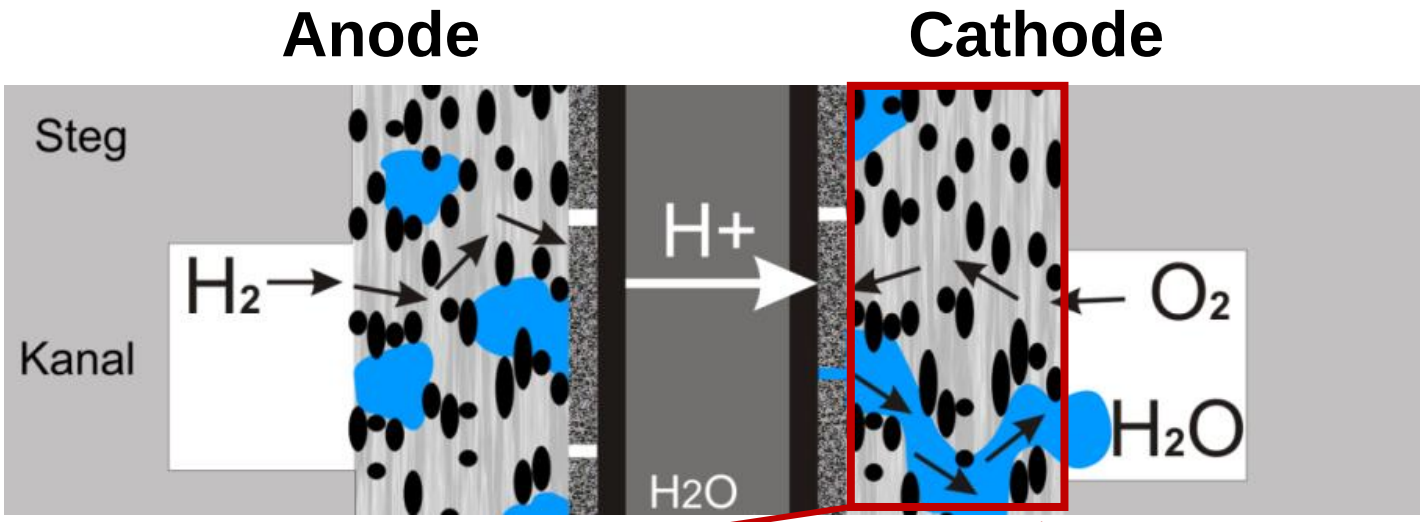

Innovative design

Hydrophobic material

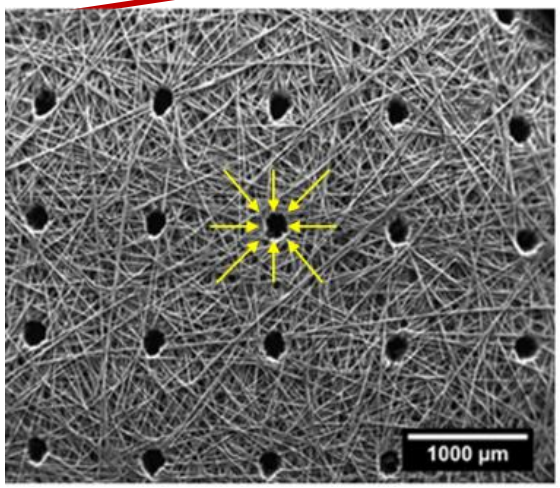

Perforation = Drainage effect

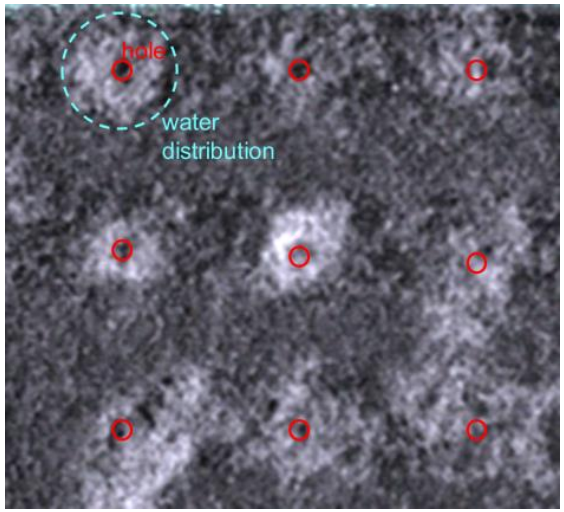

Neutron image

BER II

Attenuation Contrast

Fuel Cells

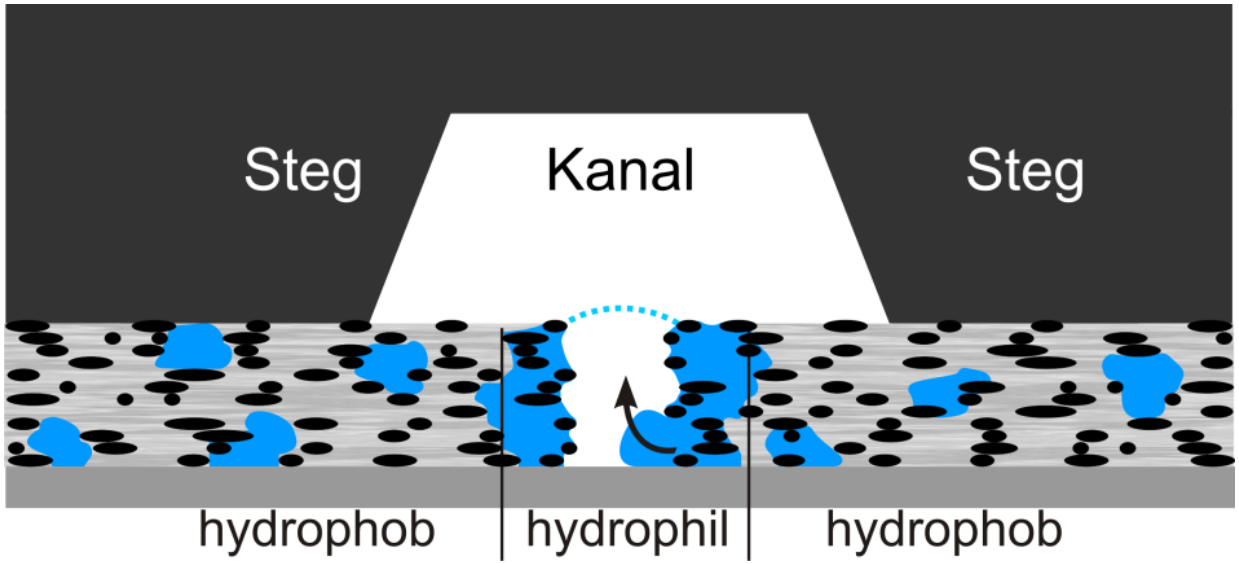

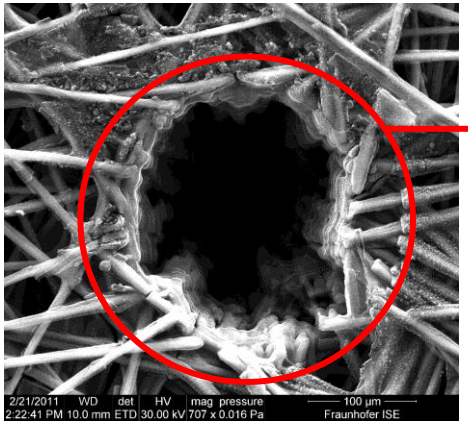

Heat affected zone

Hydrophilic areas cause water agglomerations

Attenuation Contrast

Fuel Cells

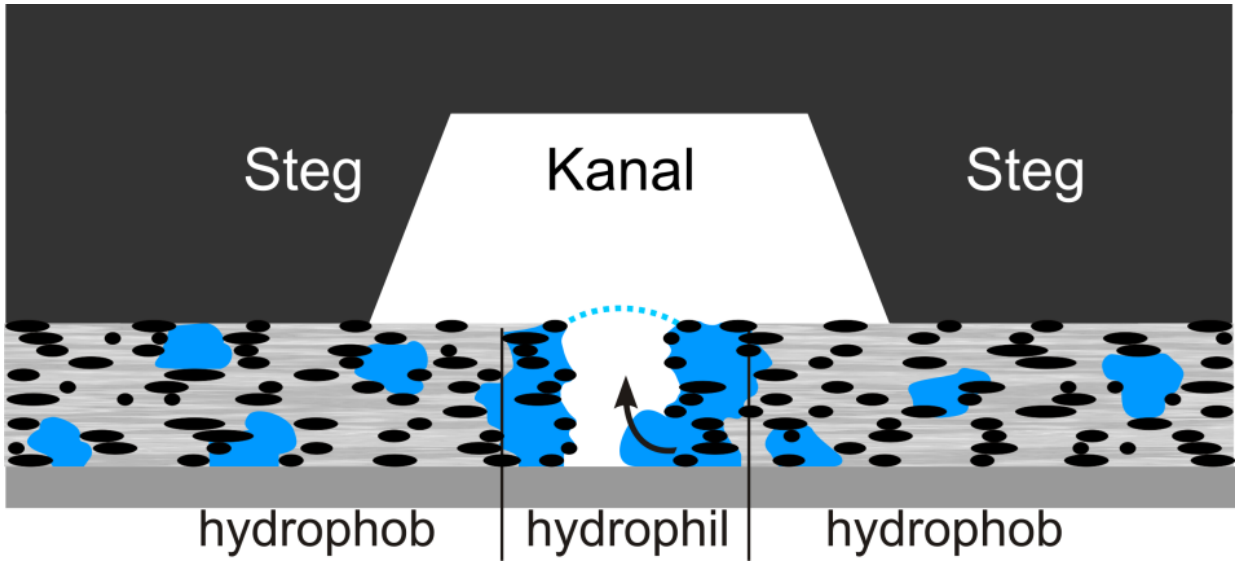

BESSY II

laser perforation

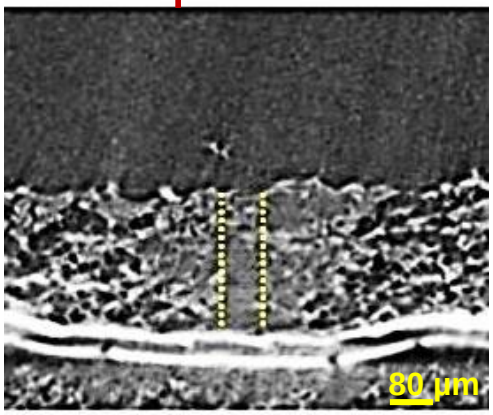

mechanic perforation

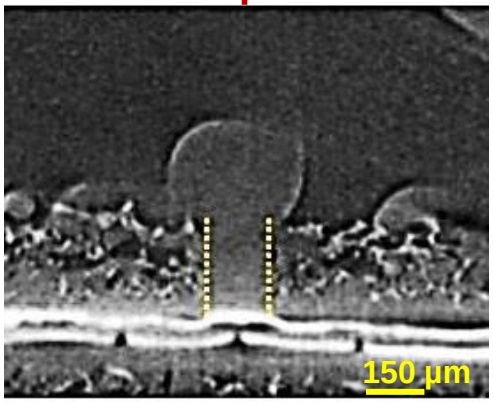

dynamic synchrotron radiography

Attenuation Contrast

Fuel Cells

Best case: 40% performance increase
Typical: 10-20% increase

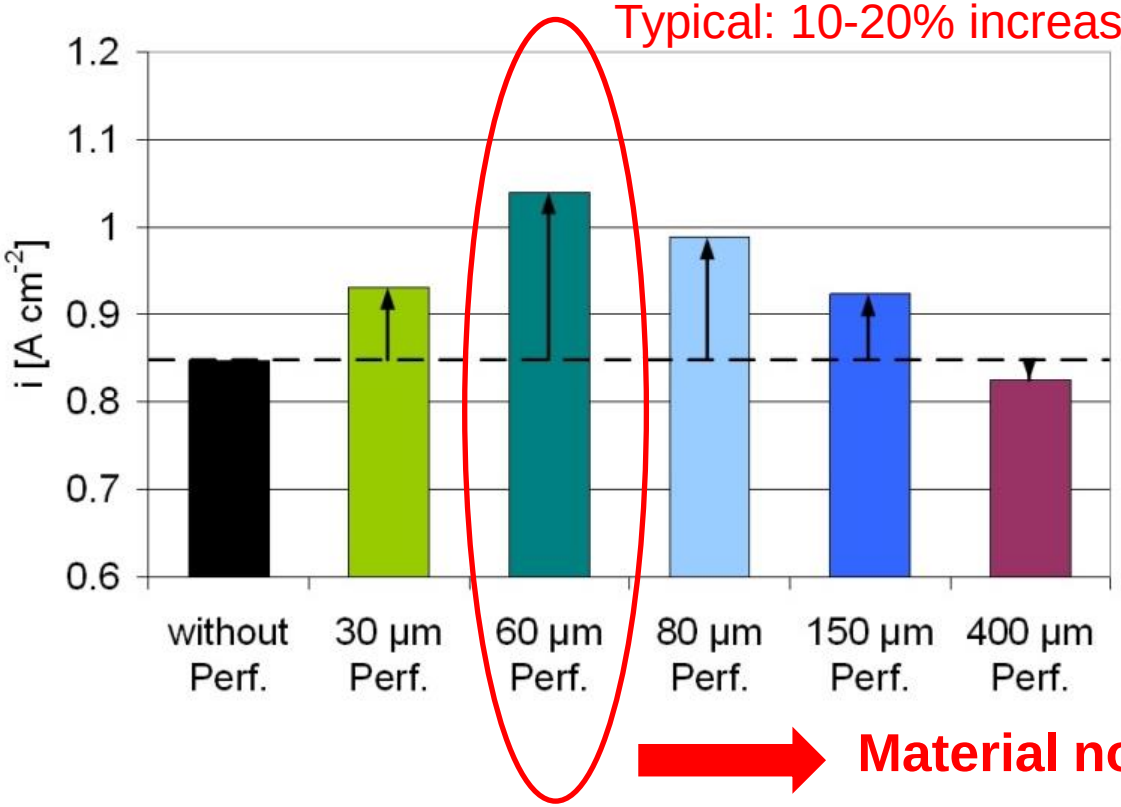

Material now in production

J. Haußmann *et al*
Journal of Power Sources 239 (2013) 611

Al-alloy +TiB_2 foam

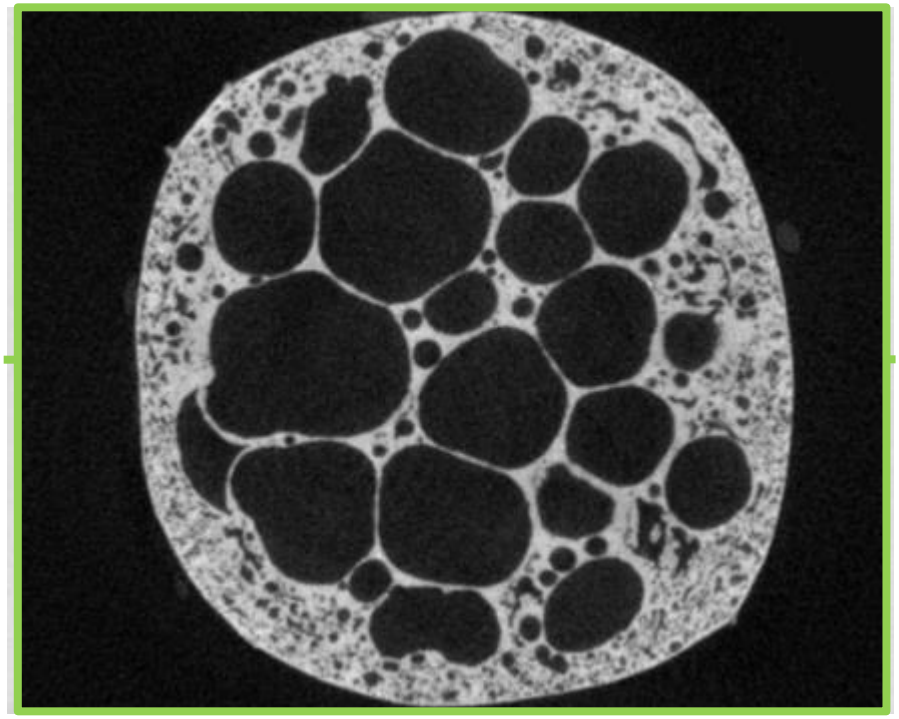

X-rays, 120 kV
Pixel size: 15 µm (resolution: 20 µm)
Flat panel

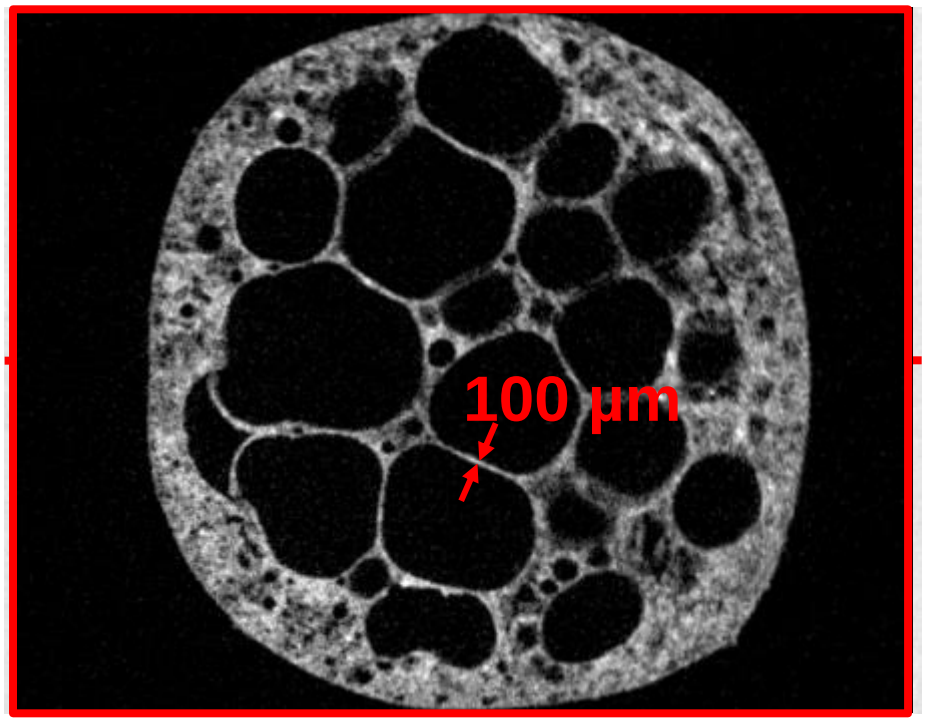

Cold neutrons
Pixel size: 13.5 µm (resolution: 30 µm)
Gadox 10 µm
Lens system: 200mm

SiO_2 particles in water

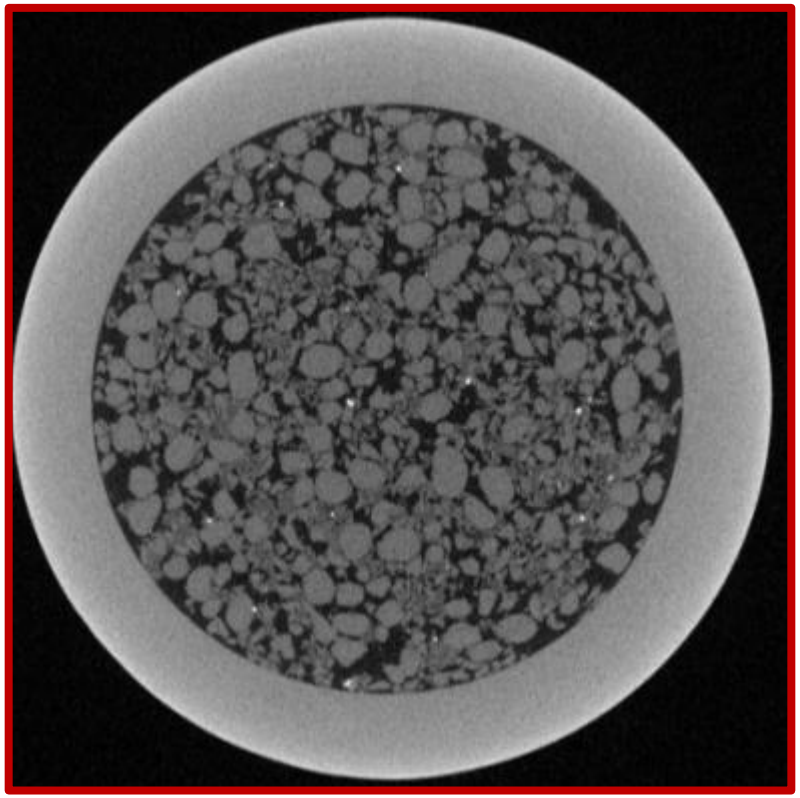

X-rays, 120 kV
Pixel size: 15 µm

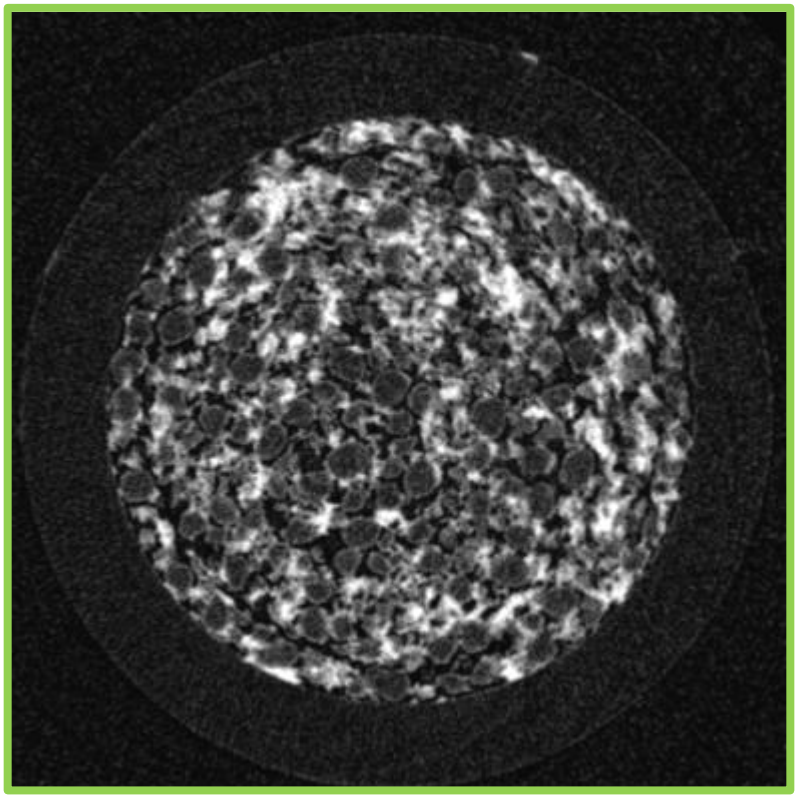

Cold neutrons
Pixel size: 13.5 µm (resolution: 30 µm)
Gadox 10 µm
Lens system: 200mm

Kim, Felix Hoyean. "Dual-Modality (Neutron And X-Ray) Imaging For Characterization Of Partially Saturated Granular Materials And Flow Through Porous Media." (2013).

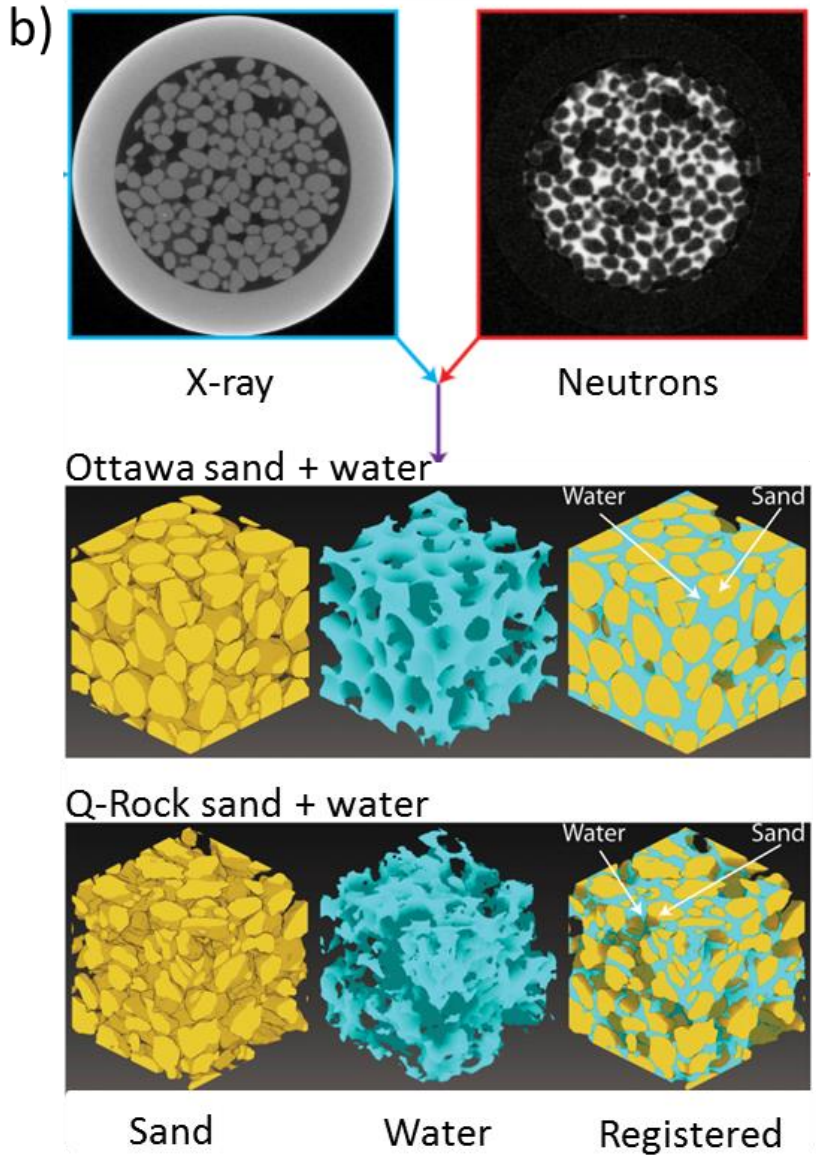

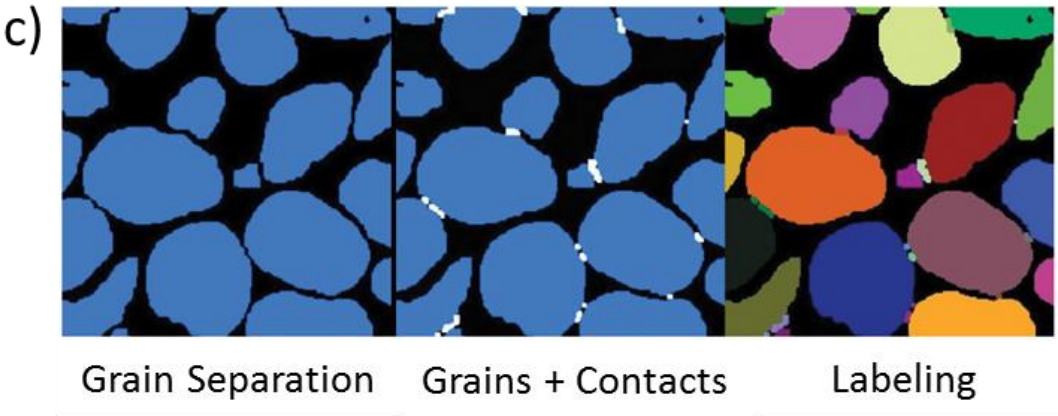

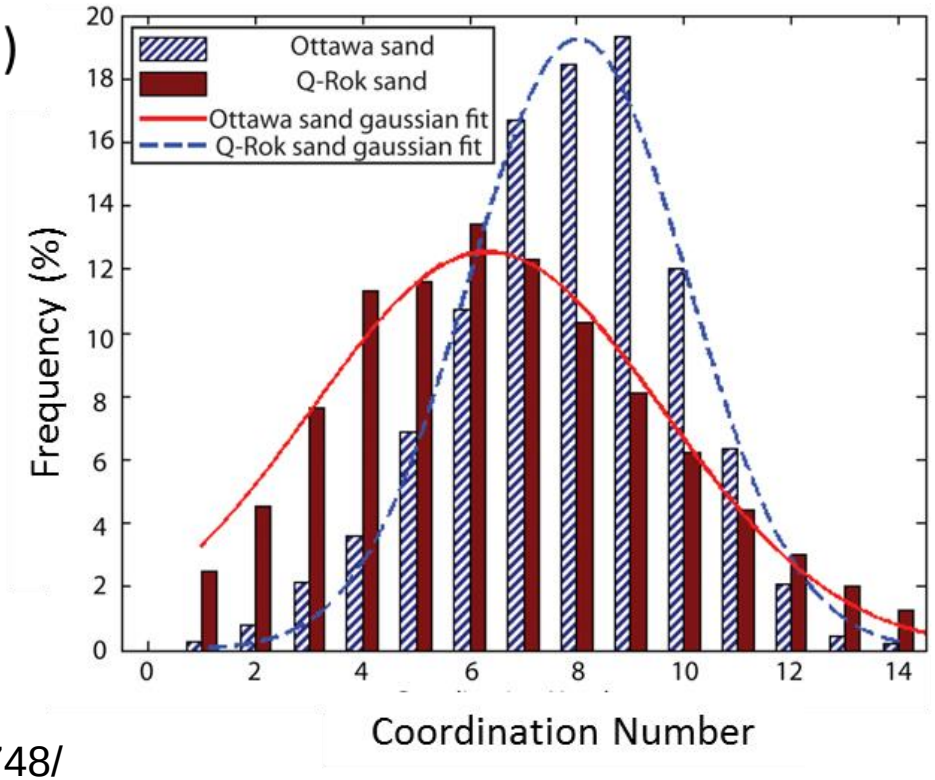

https://trace.tennessee.edu/utk_graddiss/1748/

The signal chain

Now let's do it backwards:

- We have a sample that attenuates the neutron beam by 50%.
- We want to detect a 2% variation in the sample.
  (Say, a crack or bubble within the sample.)
- This means 1% of the full neutron fluence (without sample) on one pixel.
- The poisson noise in any particle distribution is sqrt(N), and our signal must be above the noise.
- sqrt(100) =10, sqrt(1,000)= 31.6 , sqrt(10,000)=100
- so we must DETECT at least 10,000 neutrons per pixel to be equal to noise level !
- The detection efficiency of the screen is in the order of 20-30%, say 25%.
- This means we need 40,000 incoming neutrons on one pixel !

Slide courtesy: Dr. Burkhard Schillinger (FRM-II, Munich, Germany)

The signal chain

Now let's do it backwards:

- Let's say the lens system projects an area of 0.1 mm x 0.1 mm of the screen onto one pixel of 12 um x 12 um size, we detect several photons per neutron (remember: 177,000 photons are generated in the screen per detected neutron).

- So we need 40,000 neutrons per 0.1 mm x 0.1 mm, which is 40,000 x 10,000 neutrons per 1 cm^2, a total fluence of 4x 10^8n/ cm^2.

- In a beam with a neutron flux of 1 x 10^6/ cm^2s, we need 400 seconds or 6 minutes 40 seconds exposure time.

Slide courtesy: Dr. Burkhard Schillinger (FRM-II, Munich, Germany)

The signal chain

Now let's do it backwards:

- This means the dynamic resolution of neutron imaging depends on the NEUTRON statistics, and NOT on the PHOTON statistics!

- It makes no sense to employ a super light collecting lens that transmits dozens of photons per neutron – and makes the camera overflow before the required neutron statistics is reached!

- BUT the lens should collect several photons per detected neutron so that the photon statistics does not influence the neutron statistics.

Slide courtesy: Dr. Burkhard Schillinger (FRM-II, Munich, Germany)

High temporal resolution

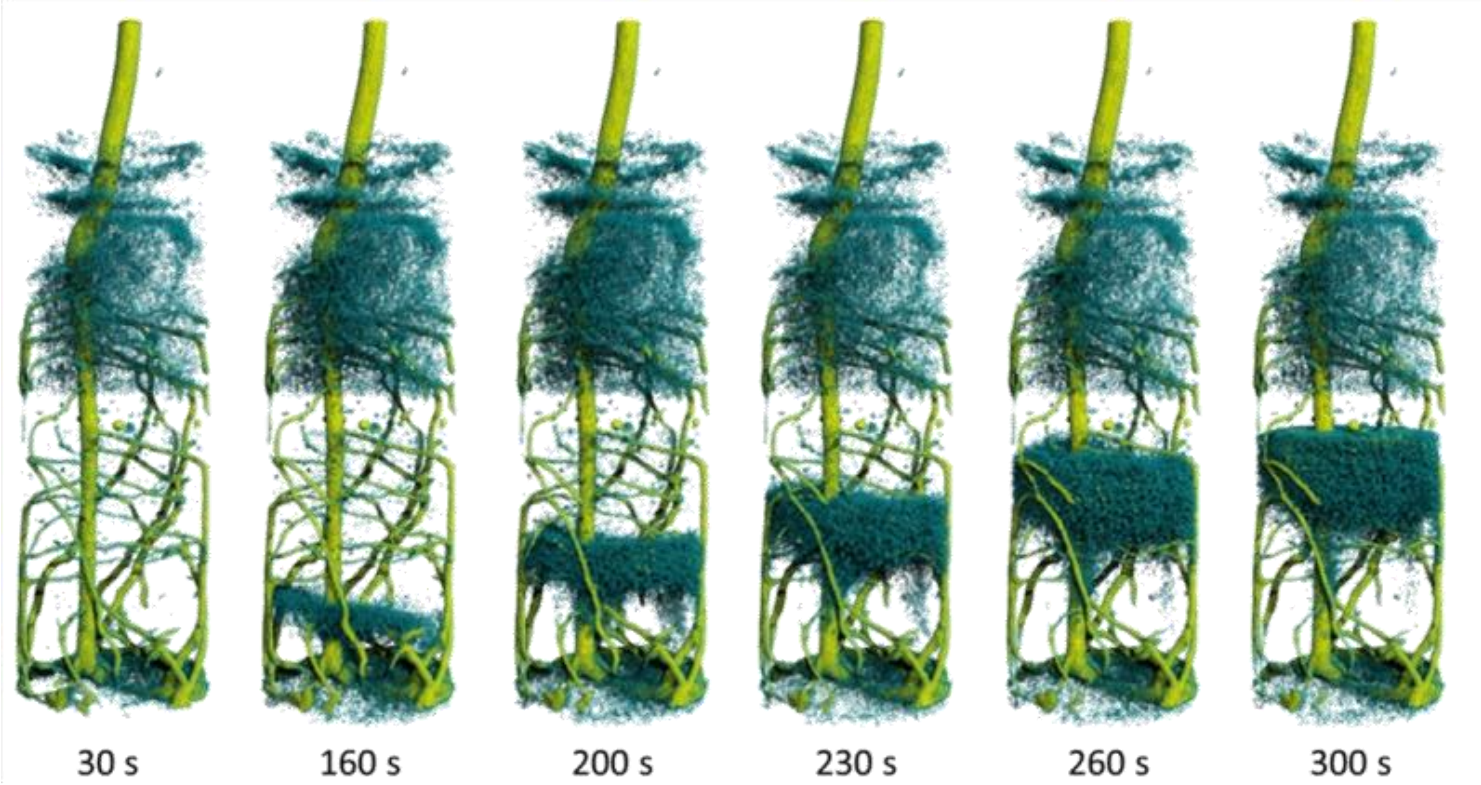

Ch. Tötzke, et al. *Scientific reports* 7.1 (2017): 6192.

Detector characterization

Exposure time readout

https://andor.oxinst.com/products/scmos-camera-series/neo-5-5-scmos

High-speed radiography

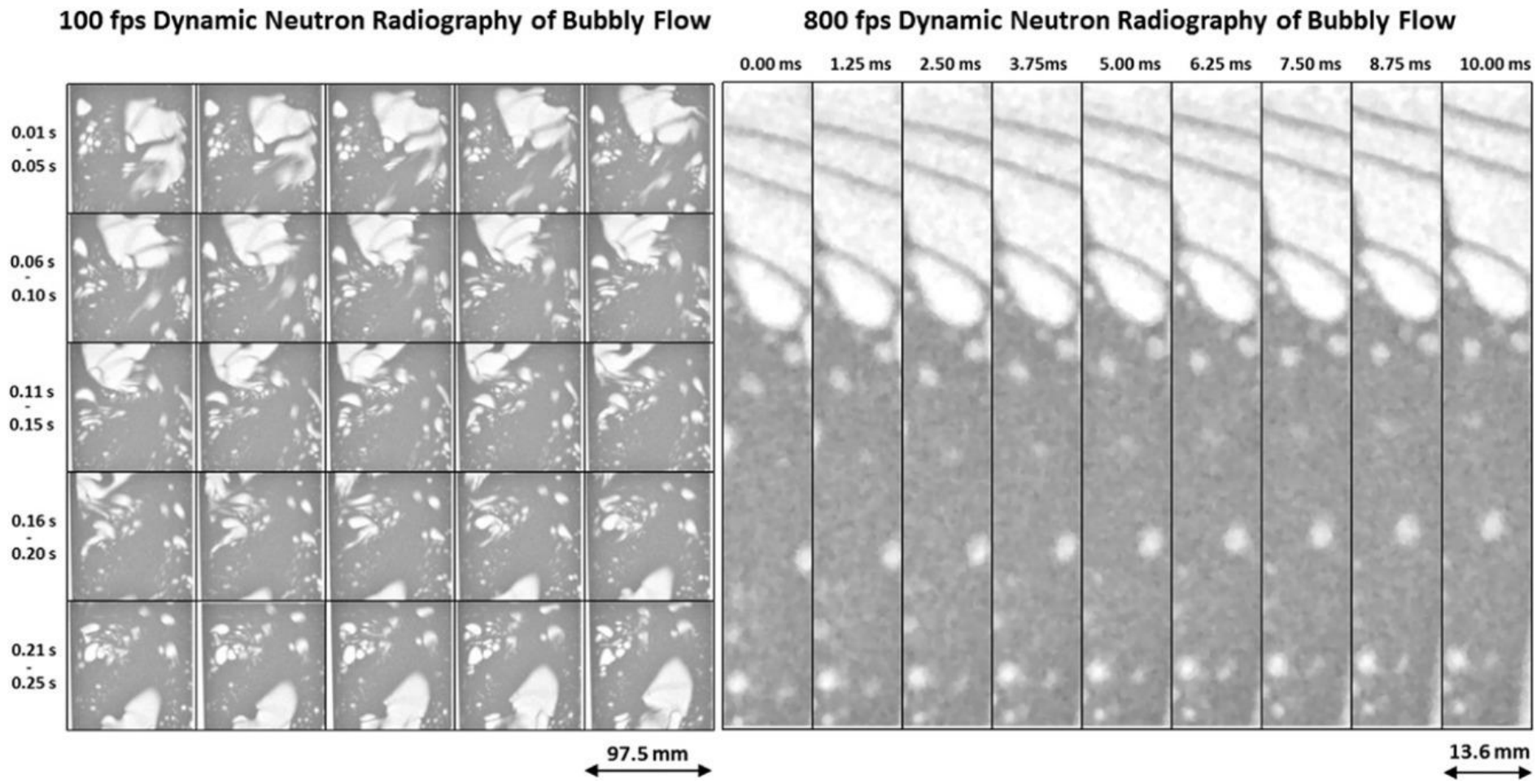

Robert Zboray, and Pavel Trtik.
"800 fps neutron radiography of air-water two-phase flow." *MethodsX* 5 (2018): 96-102.

High-speed radiography

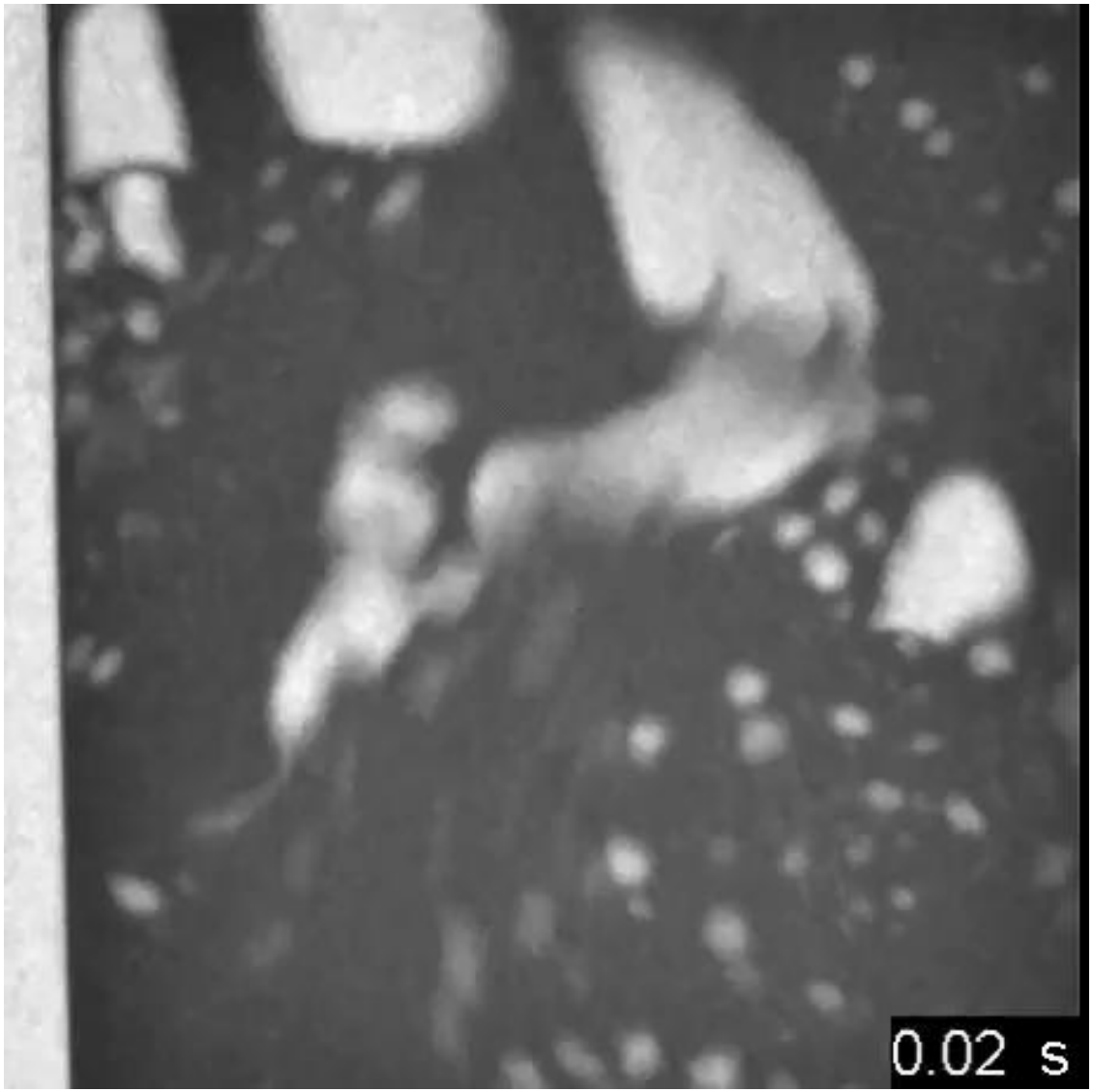

Robert Zboray, and Pavel Trtik.
"800 fps neutron radiography of air-water two-phase flow." *MethodsX* 5 (2018): 96-102.

Plant's physiology

University of Potsdam
Christian Tötzke
Sascha E. Oswald

How to observe the water uptake in plant's root

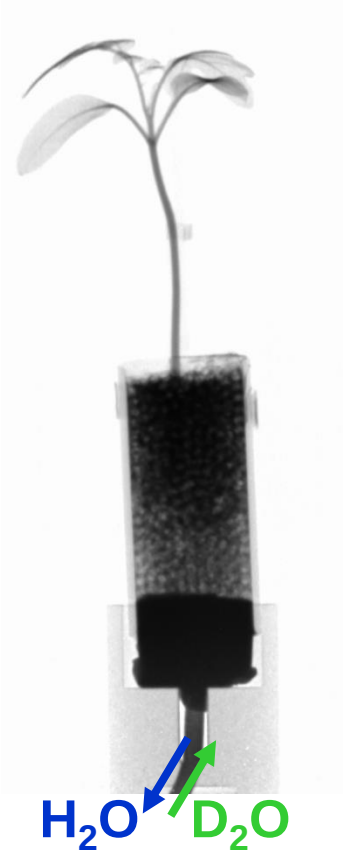

- *In-operando 3D* visualization of water distribution

Water uptake dynamics revealed with D-H contrast

Insights in the water uptake mechanisms in the root system

➔ Observation of the dynamic processes in root system

➡ Learning about the root-soil interaction mechanisms

Plant's physiology

University of Potsdam
Christian Tötzke
Sascha E. Oswald

How to observe the water uptake in plant's root

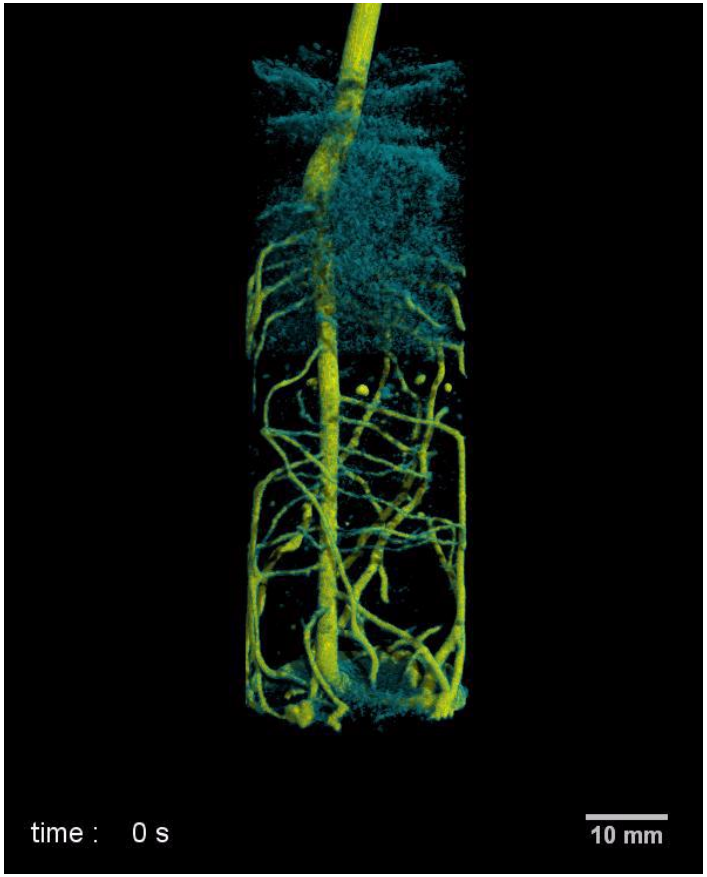

High-speed (on-the-fly) neutron tomography

resolution: 150 µm
exposure: 0.05 s
200 projections/180°

10 s / tomography

➔ Observation of the dynamic processes in root system

➔ Learning about the root-soil interaction mechanisms

Plant's physiology

University of Potsdam
Christian Tötzke
Sascha E. Oswald

How to observe the water uptake in plant's root

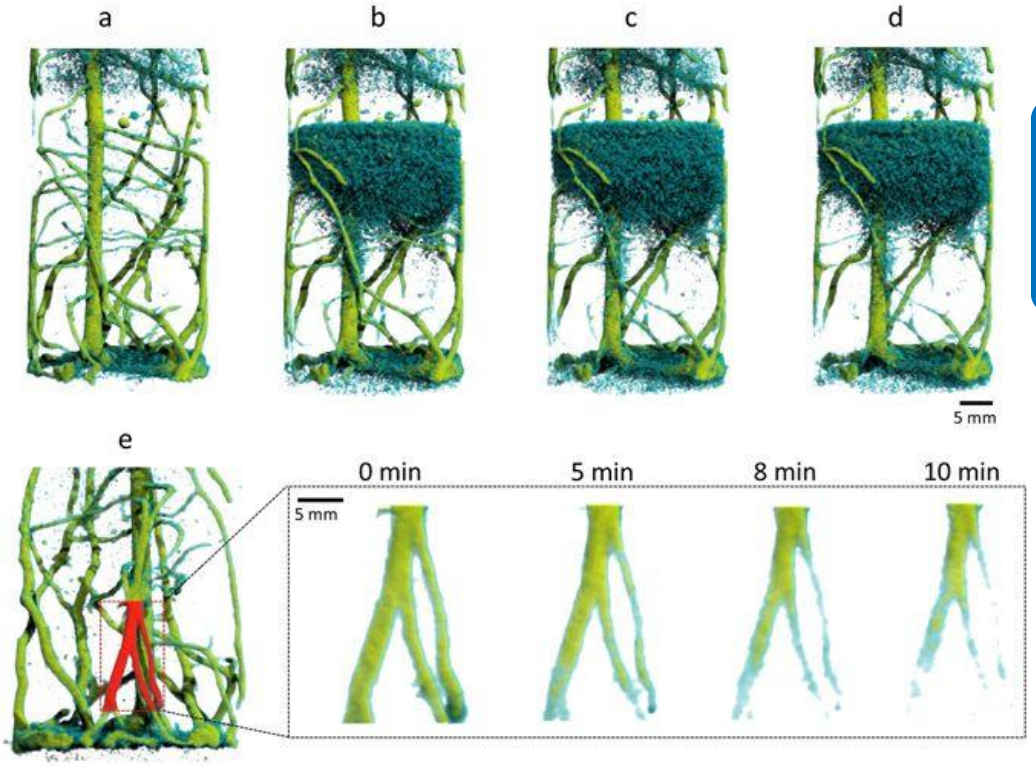

Time series of neutron tomograms at (a) 0 min; (b) 5 min; (c) 8 min and (d) 10 min after feeding D_2O.

High-speed (on-the-fly) neutron tomography

resolution: 150 µm
exposure: 0.05 s
200 projections/180°

10 s / tomography

Ch. Tötzke, et al. *Scientific reports* 7.1 (2017): 6192.

➔ **Observation of the dynamic processes in root system**

➡ **Learning about the root-soil interaction mechanisms**

Plant's physiology

Recent experiments at ILL with 3 s / tomography

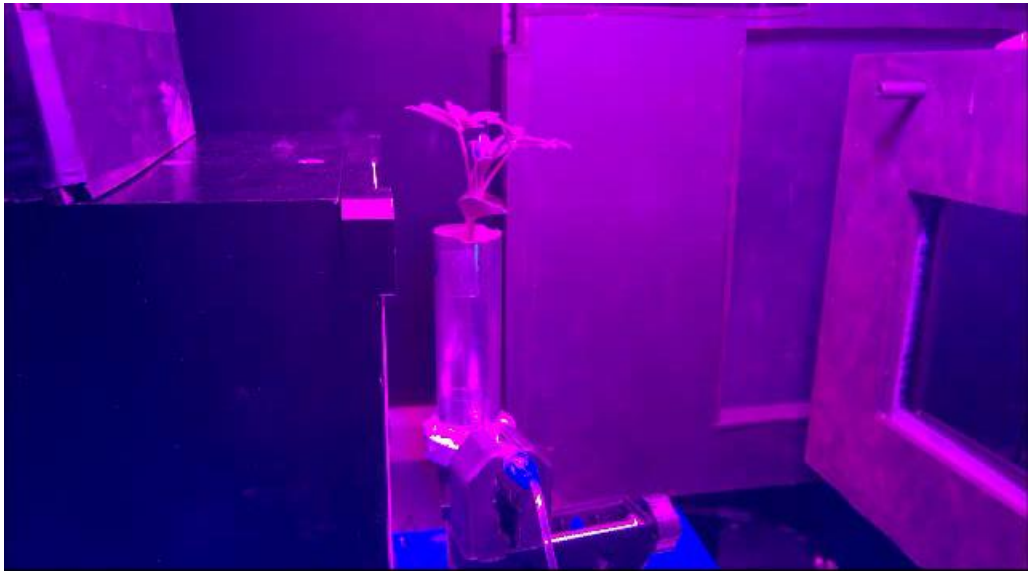

Problems:

- Speed of the rotation table
- Detector read-out time

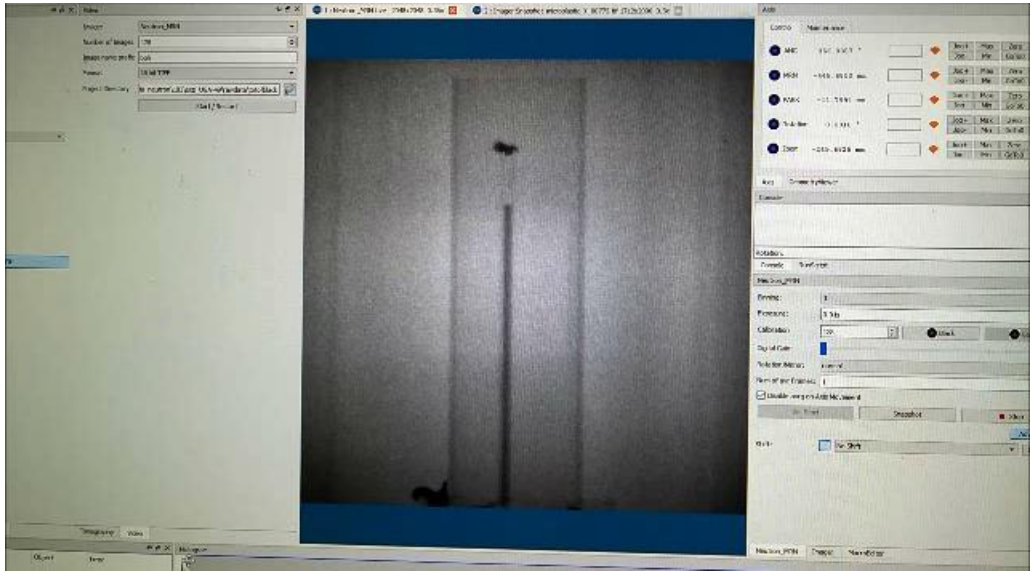

Higher power output in Fuel Cells by *innovative electrode* design

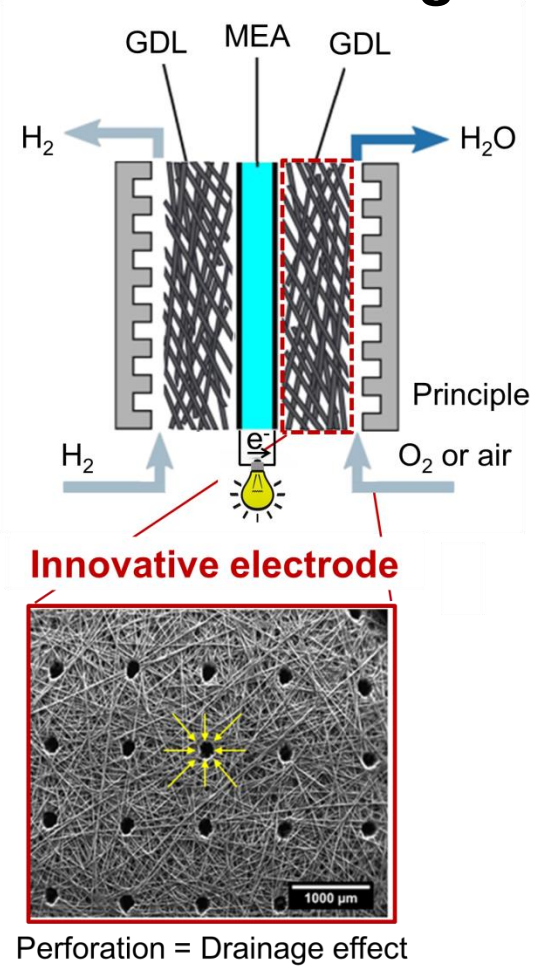

Perforation = Drainage effect

Higher hydrogen production in Electrolyser Cells by *optimized electrode*

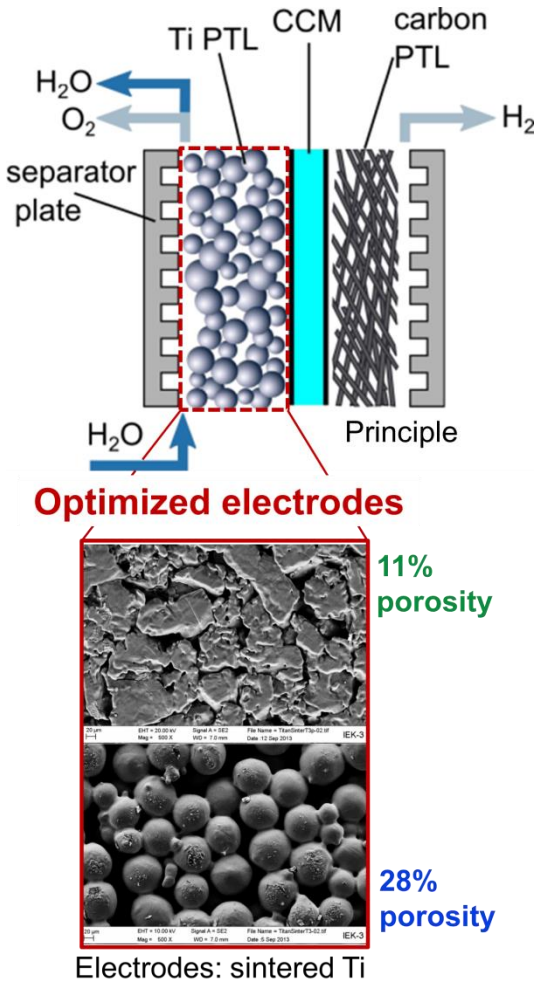

Electrodes: sintered Ti

ELECTROLYSER RESEARCH

JÜLICH FORSCHUNGSZENTRUM

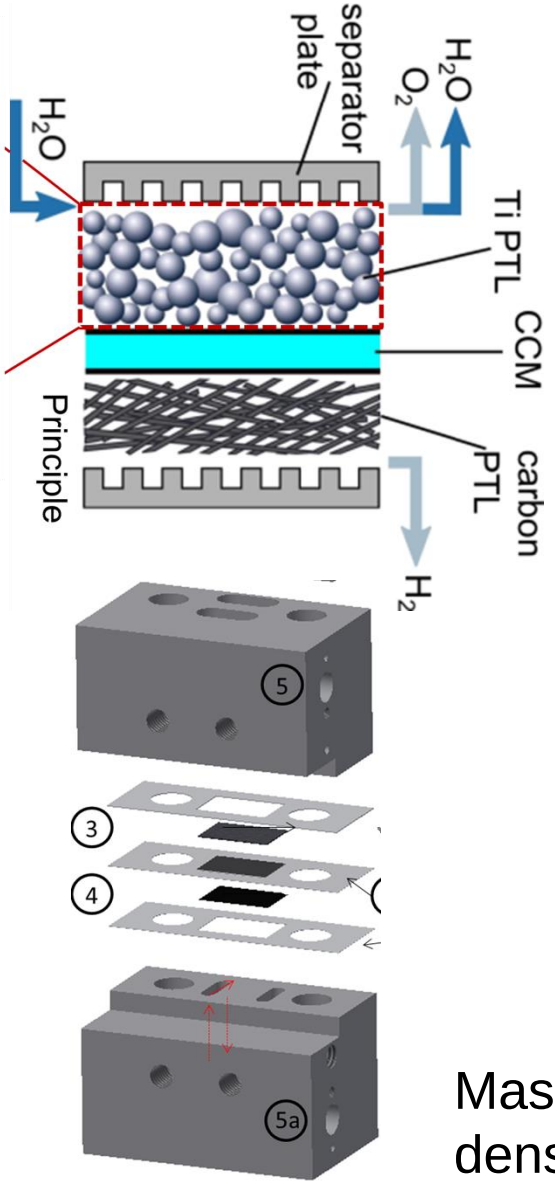

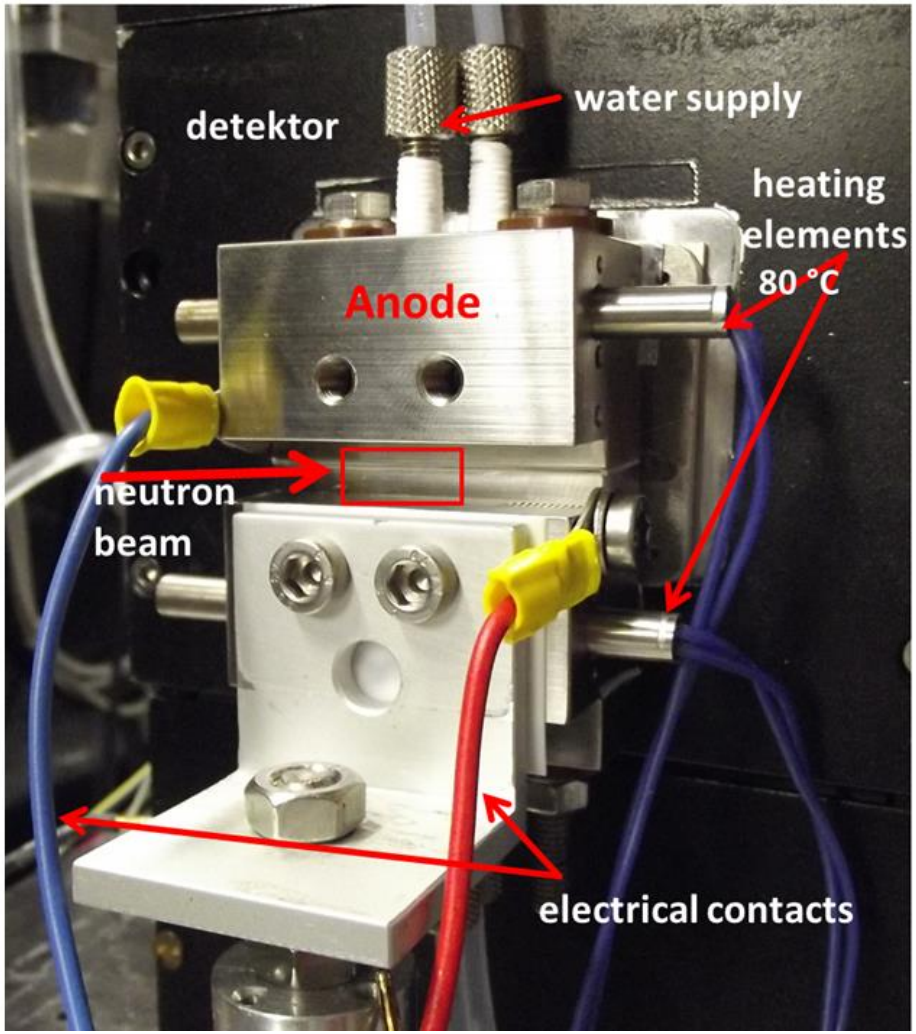

Mass transport limitation (MTL) - occurs at higher current densities and leads to a sudden increase in cell potentials

O. Panchenko *et al.* Journal of Power Sources 390 (2018)

ELECTROLYSER RESEARCH

JÜLICH FORSCHUNGSZENTRUM

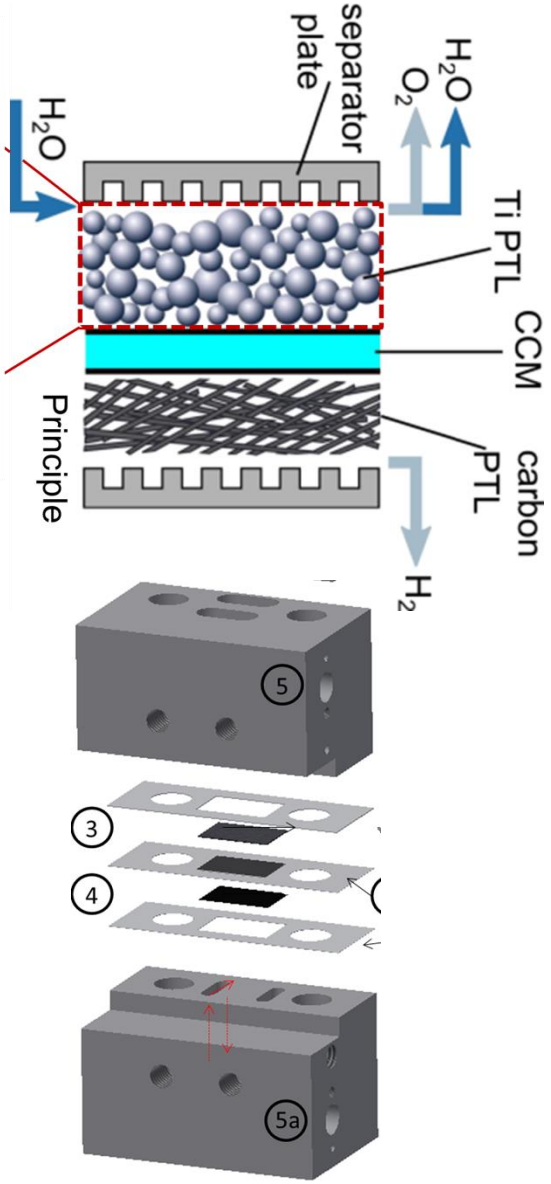

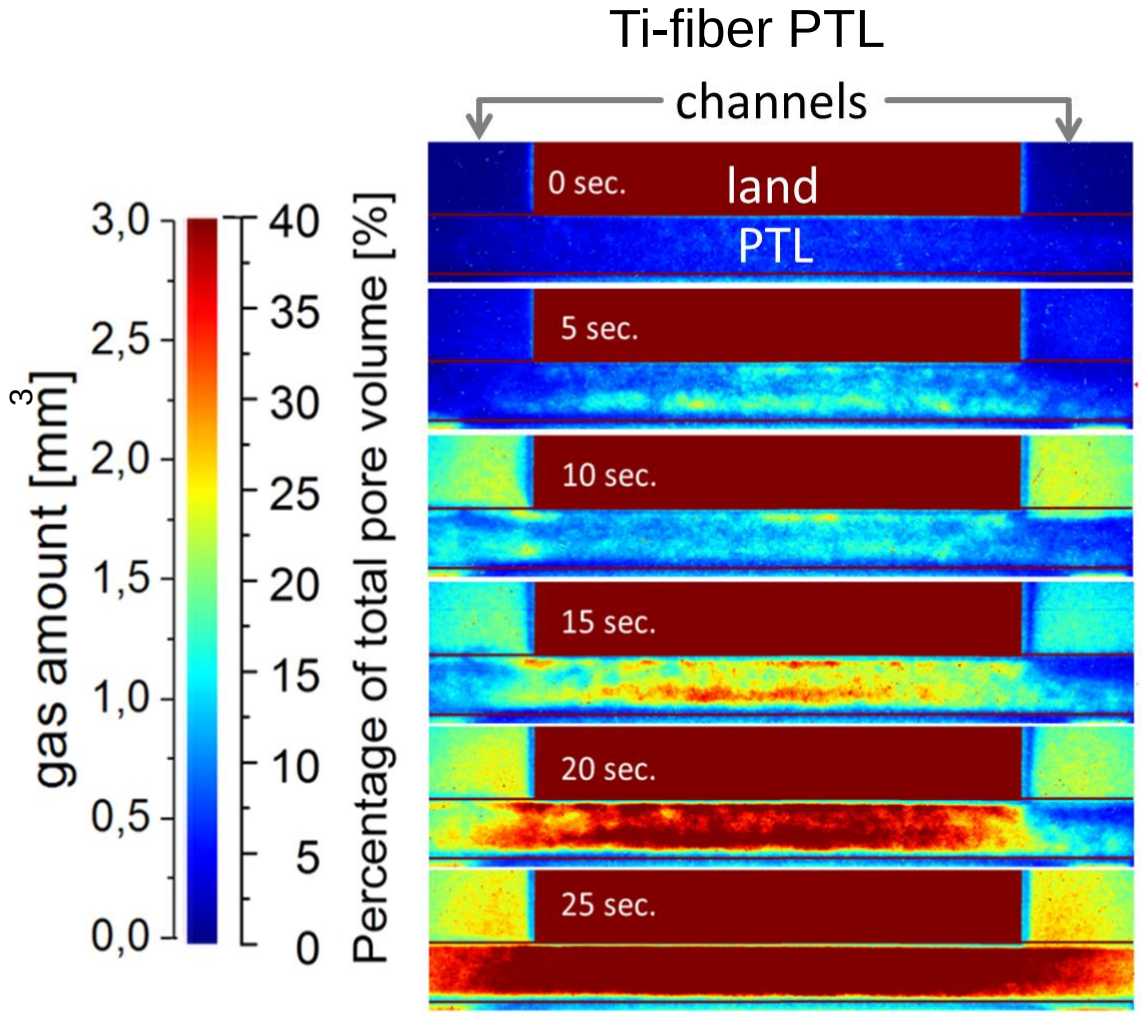

Gas distribution at voltage jump from 0 V to 1.4 V.
(Pixel size: 6.5 µm, Exposure: 5 s)

O. Panchenko *et al.* Journal of Power Sources 390 (2018)

ELECTROLYSER RESEARCH

JÜLICH FORSCHUNGSZENTRUM

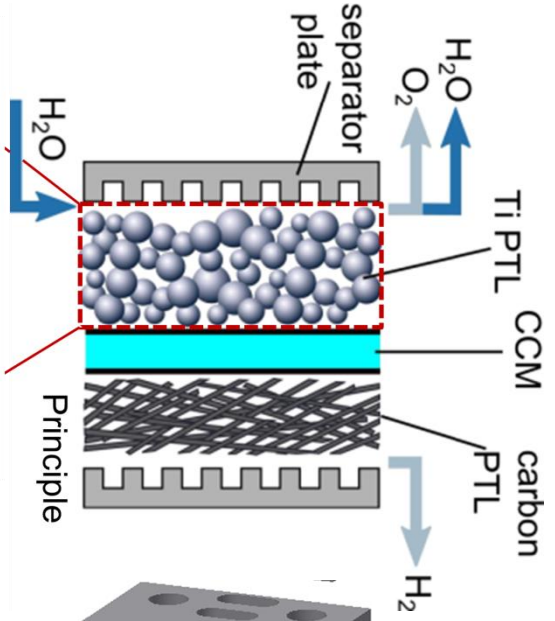

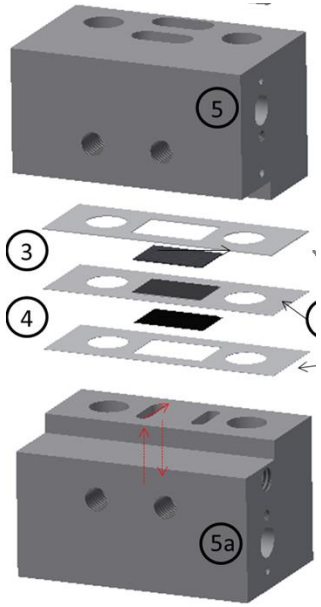

Ti-sintered powder PTL

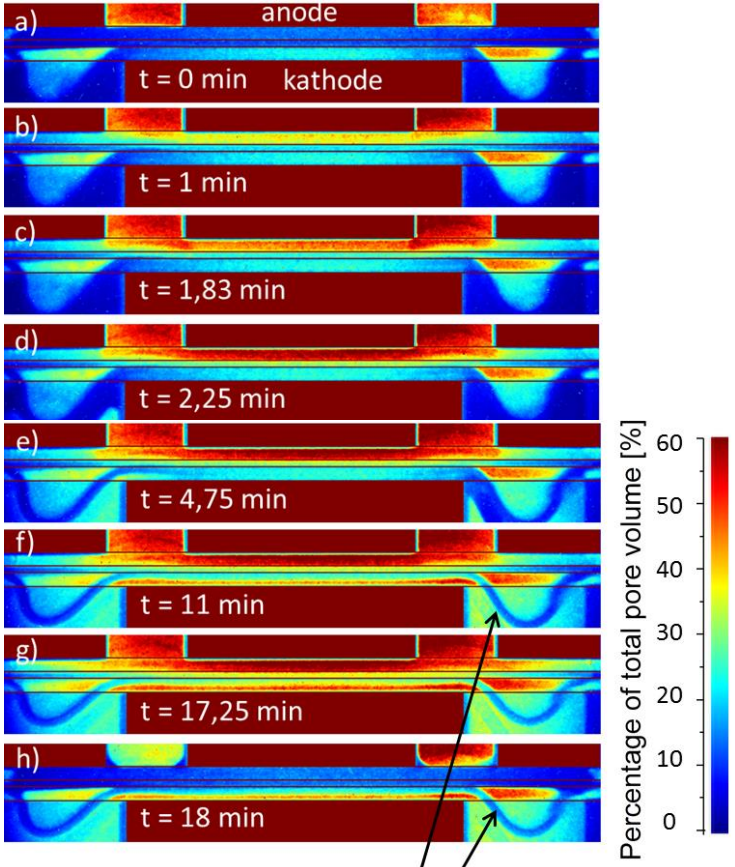

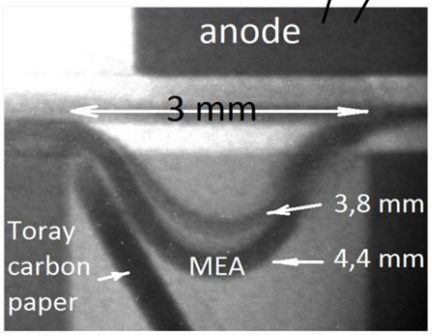

iii)

ELECTROLYSER RESEARCH

JÜLICH FORSCHUNGSZENTRUM

Ti-fiber PTL

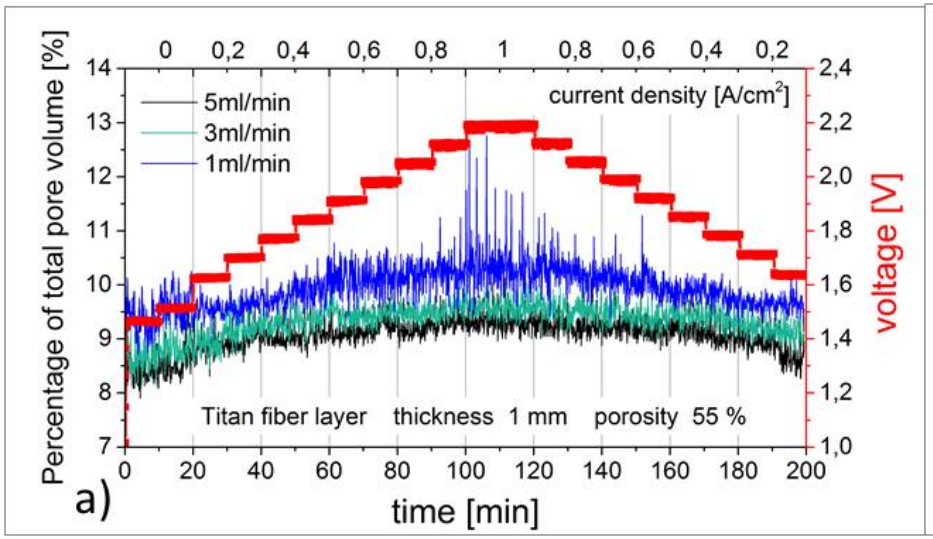

Ti-sintered powder PTL

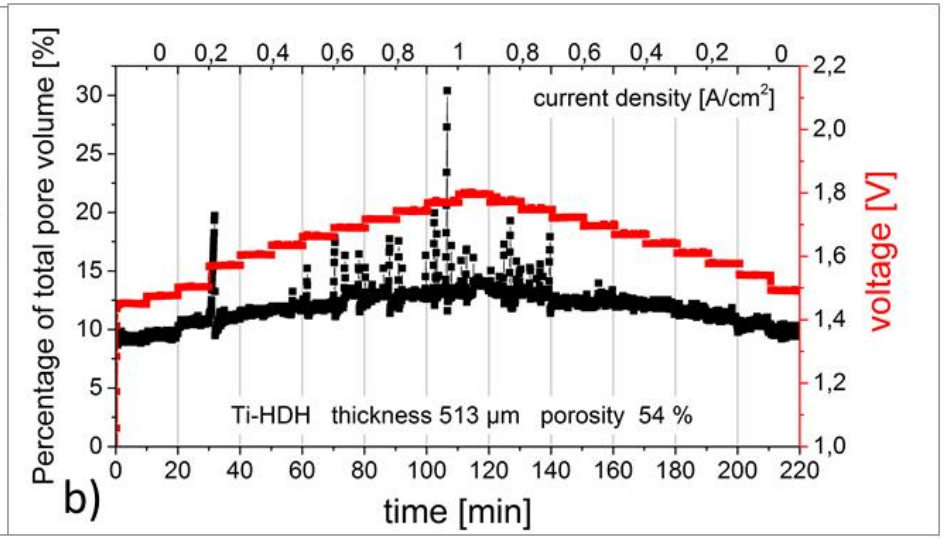

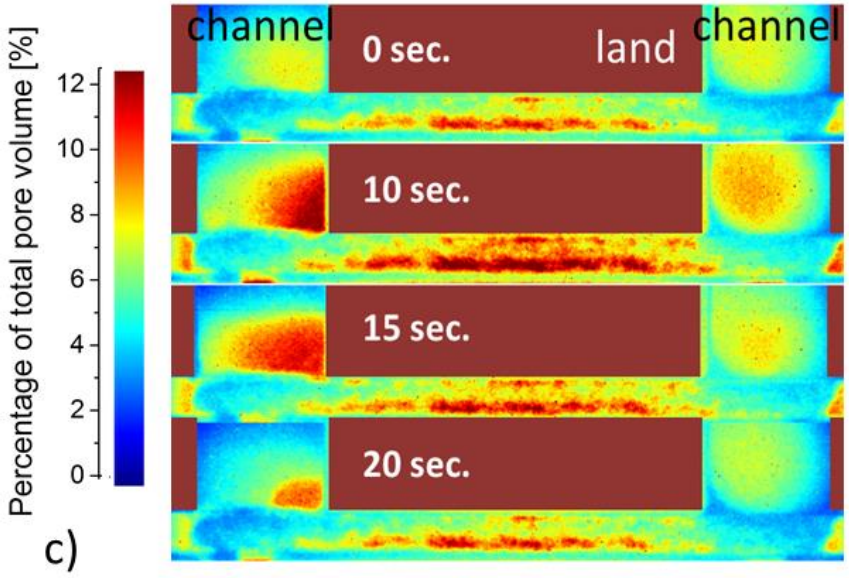

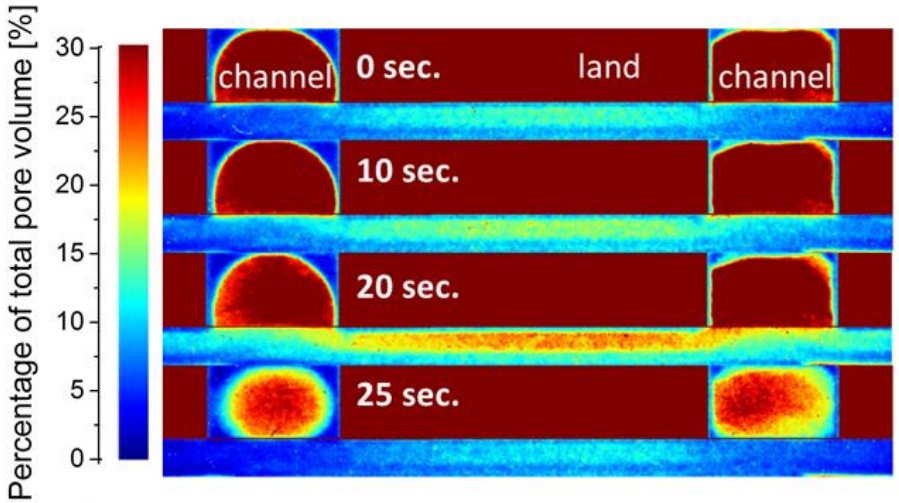

(Pixel size: 6.5 µm, Exposure: 5 s)

Large samples

Extreme samples

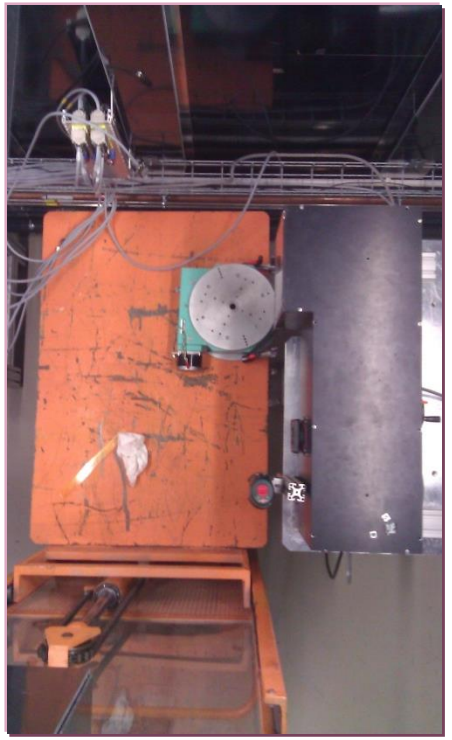

Extreme samples

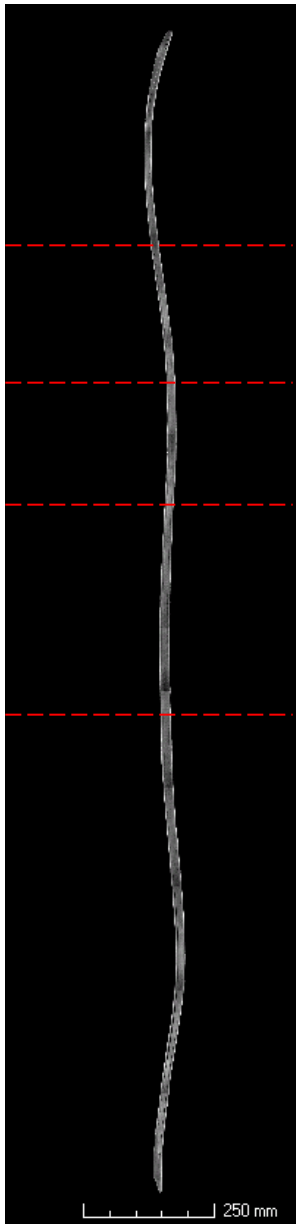

2500 mm

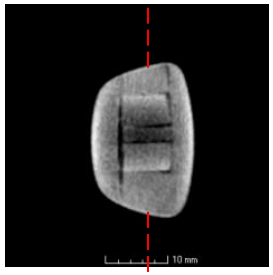

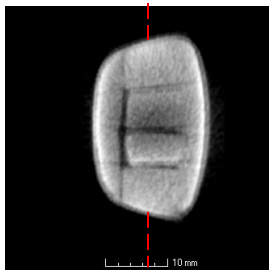

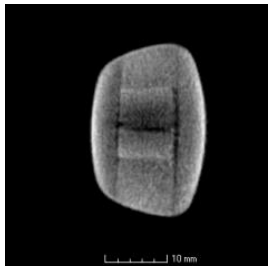

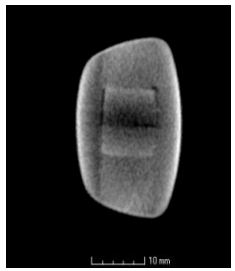

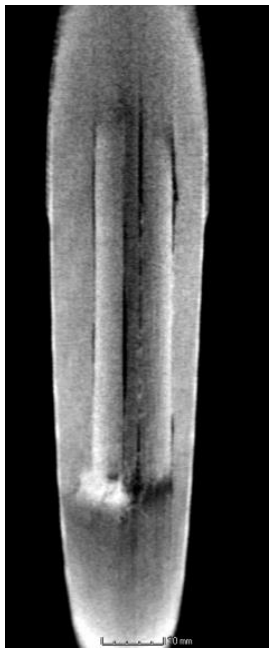

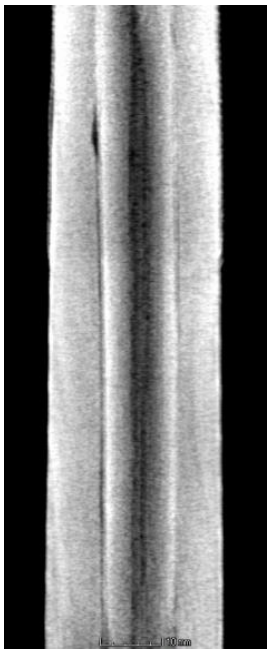

Attenuation Contrast

Shipwrecks

http://mapsontheweb.zoom-maps.com/image/64197912527

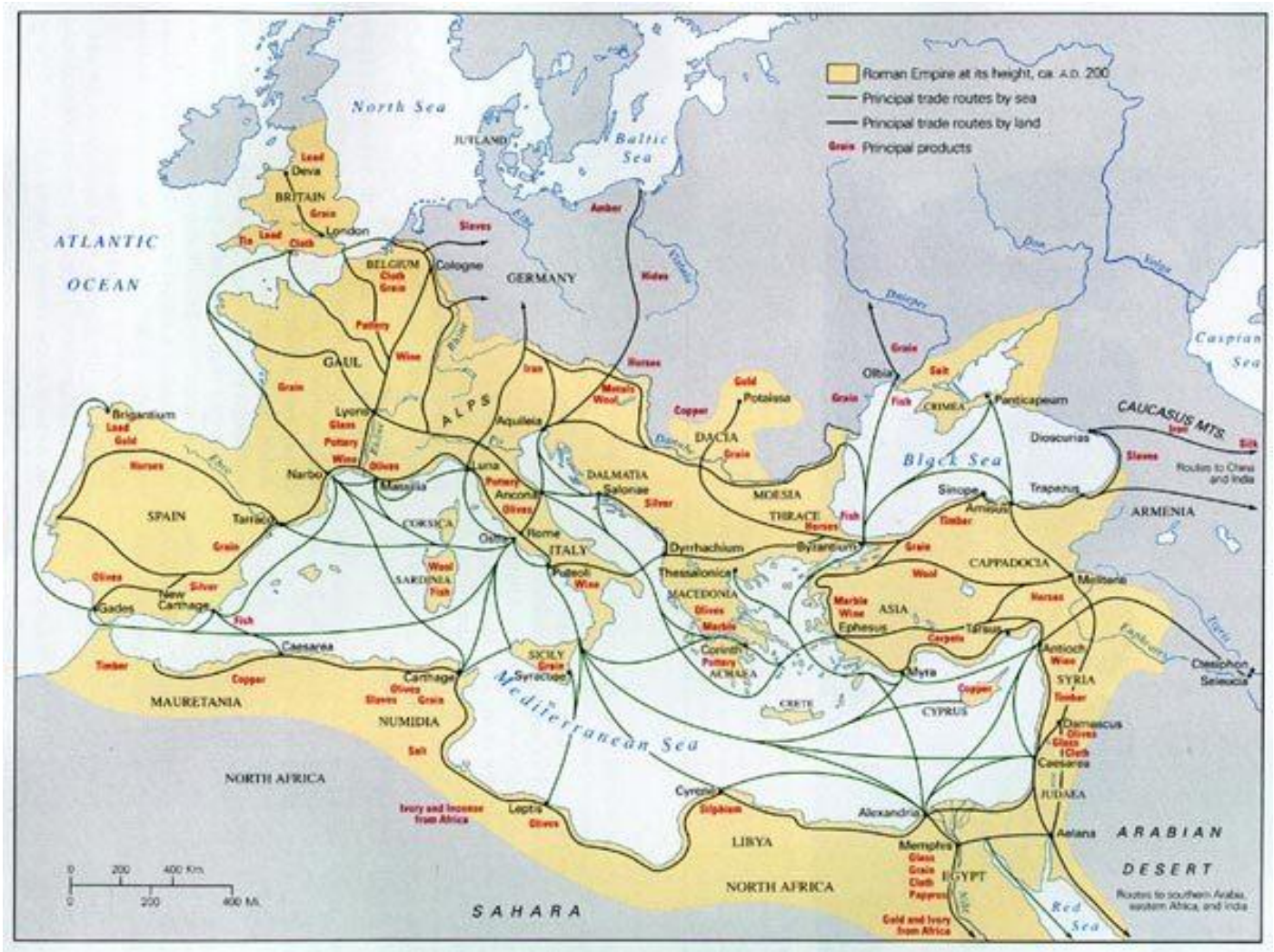

All routes lead to Rome: A map of Roman ports and trade routes

Attenuation Contrast

Lead blocks recovered near the UNESCO World Heritage Site Syracuse.
Presumably I century A.D. (Roman Imperial Age).

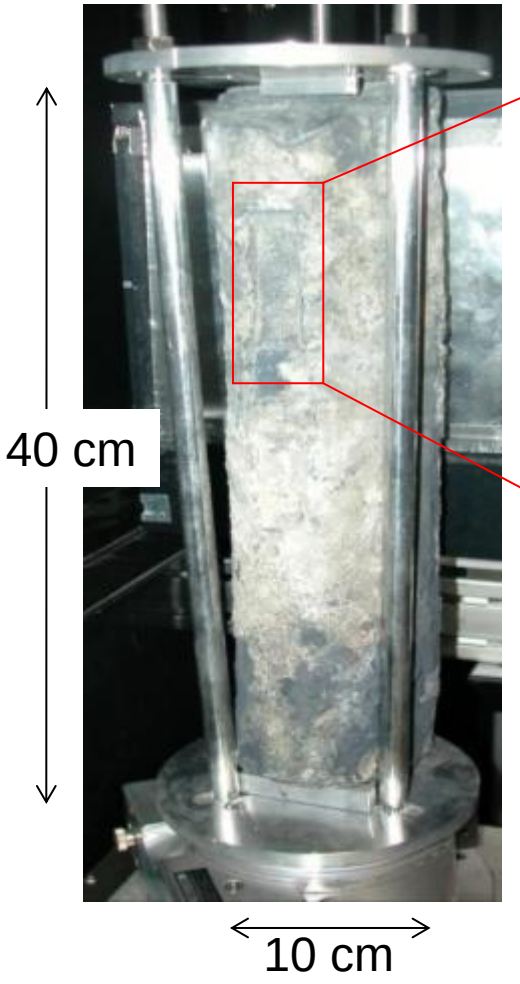

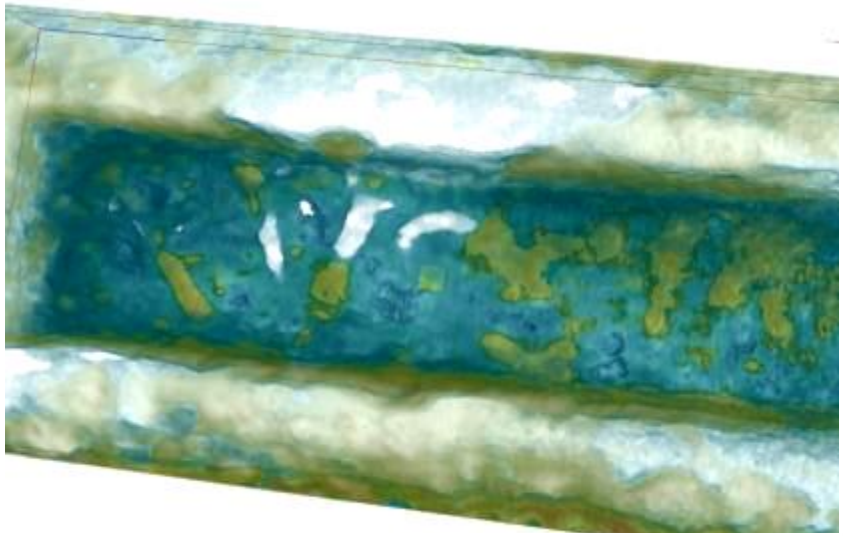

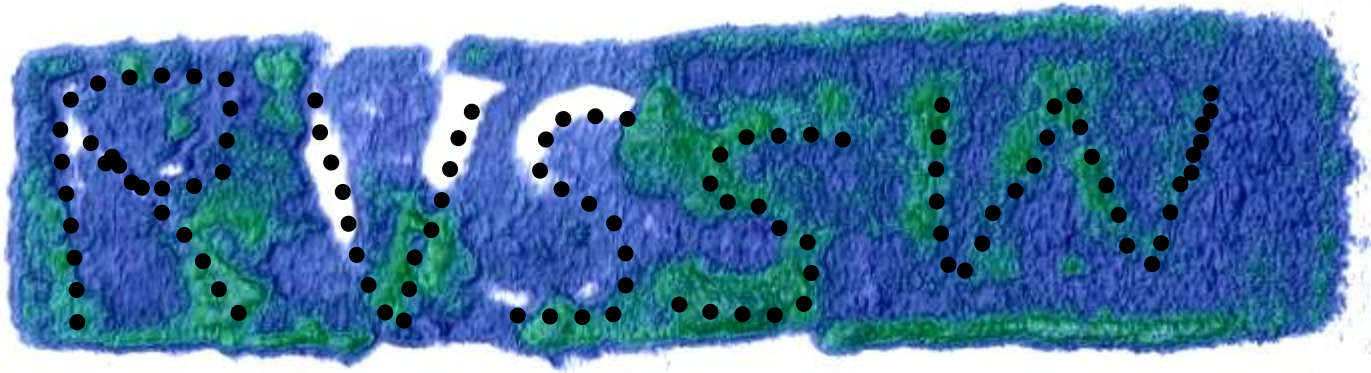

Triolo, R., et al. "Neutron tomography of ancient lead artefacts." *Analytical Methods* 6.7 (2014): 2390-2394.

Attenuation Contrast

Lead blocks recovered near the UNESCO World Heritage Site Syracuse.
Presumably I century A.D. (Roman Imperial Age).

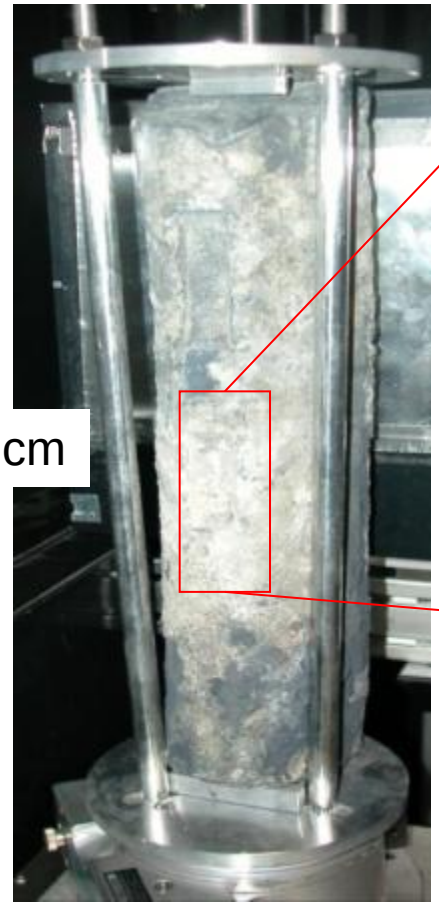

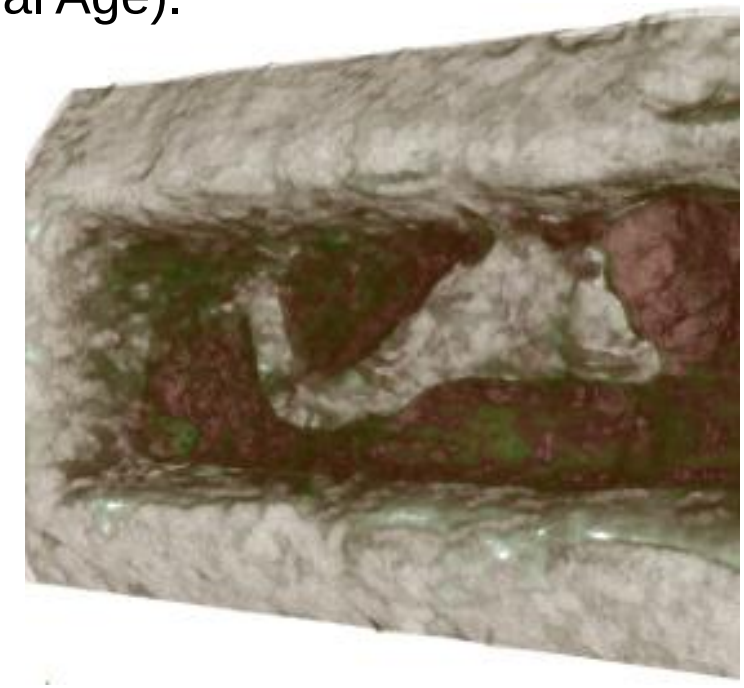

Triolo, R., et al. "Neutron tomography of ancient lead artefacts." *Analytical Methods* 6.7 (2014): 2390-2394.

Neutron tomography of bronze statues

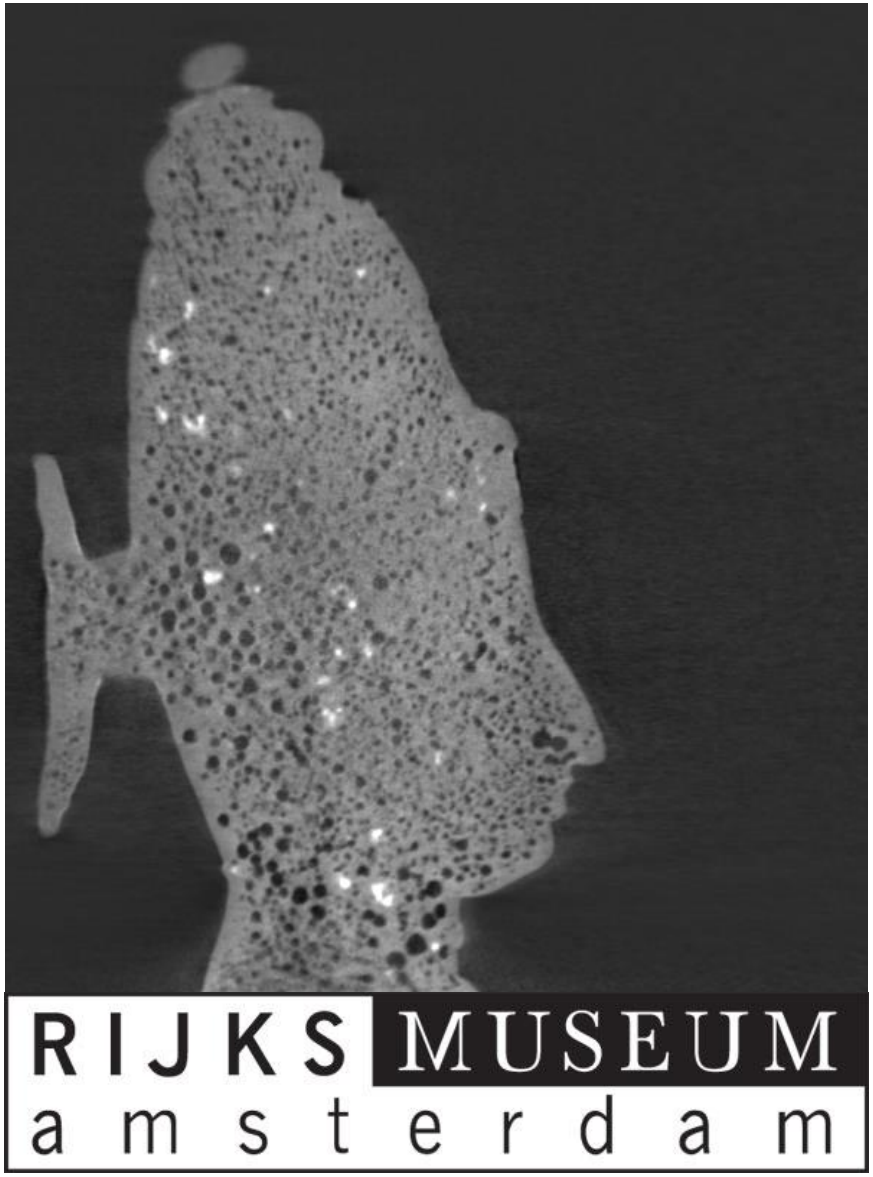

https://indico.kfki.hu/event/518/contributions/1012/

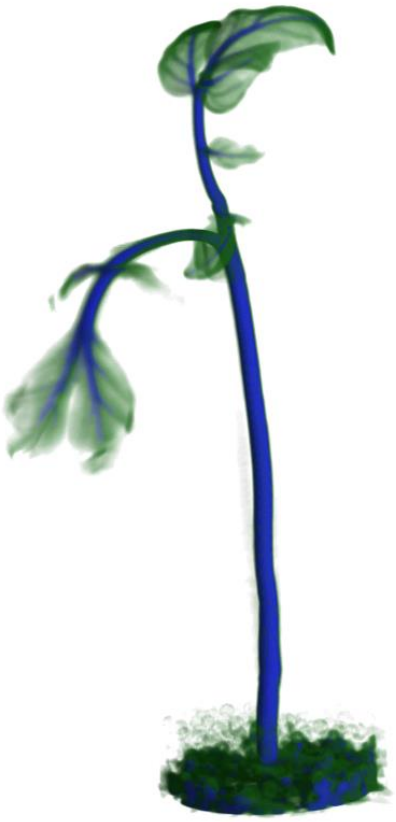

Thank you !